SYNTHESIS OF LANTHANUM OXIDE DOPED POLYANILINE NANOCOMPOSITES FOR SUPERCAPACITOR APPLIACATIONS

A DISSERTATION SUBMITTED FOR THE PARTIAL FULFILLMENTS OF THE REQUIREMENTS FOR THE MASTERS DEGREE IN CHEMISTRY

Submitted By

Prem Gaudel

Exam Roll No.: 464/072

(T.U. Regd. No.: 5-2-50-391-2011)

CENTRAL DEPARTMENT OF CHEMISTRY

INSTITUTE OF SCIENCE AND TECHNOLOGY

TRIBHUVAN UNIVERSIT, KIRTIPUR, KATHMANDU, NEPAL

October, 2020

BOARD OF EXAMINER AND CERTIFICATE OF APPROVAL

This dissertation work entitled, “**SYNTHESIS OF LANTHANUM OXIDE DOPED POLYANILINE NANOCOMPOSITES FOR SUPERCAPACITOR APPLIACATIONS’’** submitted by Mr. Prem Gaudel (Roll No. 464/072, T.U. Regd. No. 5-2-50-391-2011) has been accepted as partial fulfillment of the requirements for the Degree of Master of Science in Chemistry

……………………………….

Supervisor

Prof. Dr. Amar Prasad Yadav

Central Department of Chemistry

Tribhuvan University

………………………	……..…………………
External Examiner	**Internal Examiner**
Assoc. Prof. Dr. Surendra Kumar Gautam	Prof. Dr. Vinay Kumar Jha
Department of Chemistry	Central Department of Chemistry
Tri-Chnadra Multiple Campus	Tribhuvan University
Tribhuvan University	

…………………………….

Head of the Department

Prof. Dr. Ram Chandra Basnyat

Central Department of Chemistry

Tribhuvan University, Kirtipur

Kathmandu, Nepal

Date: October 04, 2020.

RECOMMENDATION LETTER

This is to certify that the dissertation work entitled, **"SYNTHESIS OF LANTHANUM OXIDE DOPED POLYANILINE NANOCOMPOSITES FOR SUPERCAPACITOR APPLIACATIONS''** submitted by Mr. Prem Gaudel (Roll No. 464/072, T.U. Regd. No. 5-2-50-391-2011) for the Degree of Master of Science in Chemistry of Tribhuvan University was carried out under my supervision in the academic year 2017-2019. During the research period, Mr. Prem Gaudel had performed the dissertation work sincerely and satisfactorily.

……………………….

Supervisor

Professor Dr. Amar Prasad Yadav

Central Department of Chemistry

Tribhuvan University, Kirtipur

Kathmandu, Nepal

Date: October 04, 2020

DECLARATION

I**, Prem Gaudel**, hereby declare that the present dissertation work is done originally and has not been submitted elsewhere for any degree. Any literature, data or works done by others and cited in this dissertation has been given due acknowledgements and listed in the reference section.

……………………………..

Mr. Prem Gaudel

Central Department of Chemistry

Tribhuvan University, Kirtipur

Kathmandu, Nepal

Date: October 04, 2020

DEDICATION

Dedicated to my beloved parents

Yuddha Lal Gaudel and Bimala Gaudel

And family

ACKNOWLEDGMENTS

I express my sincere gratitude to my respected supervisor Professor Dr. Amar Prasad Yadav of Central Department of Chemistry, Tribhuvan University. I am always gratefully obligated to him for his continuous support, valuable comments, and continuous encouragement throughout this research and writing for this dissertation work.

I owe my deep gratitude to Professor Dr. Ram Chandra Basnyat, Head of Department for providing me the necessary laboratory facilities to carry out this research work.

I extend my gratitude to Assoc. Prof. Nabin Karki, Asst. Prof. Dipak Kumar Gupta, and Asst. Prof. Sanjay Singh for their consistent help and support, encouragements and insightful comments.

I would like to thank University Grants Commission, Sanothimi, Nepal for providing faculty research grant (Grant No. FRG-73/74-S&T-08).

My sincere thanks also go to all respected faculty members, entire technical and administrative staff of the Central Department of Chemistry, T.U Kirtipur and Mr. Shyam Shrestha for their suggestions and help throughout the study.

I would like to acknowledge my dear friends Krishna Prasad Gautam, Subas Pandey, Ashrap Idreese, and other friends of the Central Department of Chemistry for their continuous support for the completion of my thesis work.

Finally, I am extremely indebted to my family for their constant support and encouragement lead to the successful completion of this research work.

Prem Gaudel

ABBREVIATIONS

APS	Ammonium persulphate
CV	Cyclic Voltammetry
EDX	Energy Dispersive X-Ray Spectroscopy
ES	Emeraldine salt
LE	Leucomeraldine
NPs	Nanoparticles
NAST	Nepal Academy of Science and Technology
PG	Pernigraniline
PANI	Polyaniline
PVDF	Polyvinylidene fluoride
SC	Specific Capacitance
SCE	Standard Calomel Electrode
V	Volt
XRD	X-ray Diffraction

ABSTRACT

Lanthanum oxide was prepared by the precipitation method using EDTA solution with the $La(NO_3)_3.6H_2O$ in acidic medium in presence of 10% oxalic acid at pH of 3-4. The formation of La_2O_3 was confirmed by the XRD. The size calculation of La_2O_3 from the XRD data shows the size of 19.17 nm. The Different proportions of prepared La_2O_3 (0.1, 0.2, 0.3, 0.5 g) was doped with double distilled aniline to form PANI-La_2O_3 composite by the in situ aqueous oxidative chemical polymerization method in 1 M H_2SO_4 solution at the room temperature. The prepared composite was mixed with little carbon black and little PVDF and fed into the nickel form and then dried. These electrodes were subjected to measure various electro chemical behaviors like cyclic voltammetry and galvanic charge discharge curves. CV for the samples was taken with the scan rate of 10 mV/s. The Galvano static charge discharge cycle of samples were taken at a current of 4 Ag^{-1} in three electrode system between the potential ranges of -0.2 to 1 V. From both specific capacitances of the electrodes was studied. The specific capacitance for the sample (S_2) 0.2 gm La_2O_3 doped in PANI in 1 M H_2SO_4 has highest values of 206 Fg^{-1} that was obtained from CV. The same sample also showed the highest specific capacitance of 210 Fg^{-1} in galvanic charge discharge cycle. From these we can conclude that the sample (S_2) 0.2 gm La_2O_3 doped in PANI in 1 M H_2SO_4 will be the best among these samples for the supercapacitor applications.

TABLE OF CONTENTS

List of the Figures

List of the Tables

CHAPTER-1: INTRODUCTION

1.1 General Background

Supercapacitor are also known as ultra-capacitor as they are high capacity capacitors, it has much more capacitance then other normal capacitors, with lower voltage limits then other batteries, it has 10-100 more energy per unit volume, it can be easily charged and discharged then other electrical capacitors and can go much more cycle of charging and discharging and also stores much more energy [1].

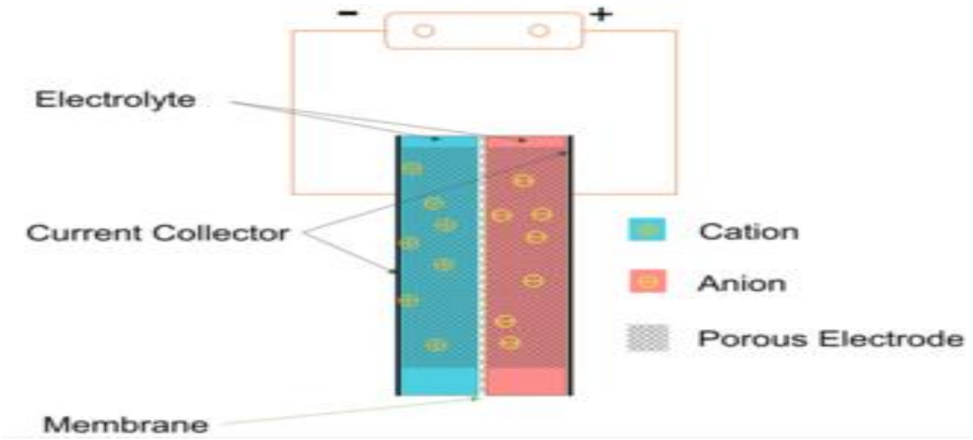

Fig: 1.1 Schematic illustration of super capacitor

Supercapacitors are emerging as devices of prime importance owing to the following advantages:

- High power densities capable of instantly charging and discharging.
- Long lifetimes capable of more than 100,000 charge–discharge cycles. Free from maintenance capable of using for a long time until abandoned.
- Excellent safety and reliability issues, low heat generation during operation, recoverable even after short-circuiting.
- Wide operational temperature ranges.
- No fear of material shortage. Activated carbon materials can be obtained from any organic substance.
- Free of heavy metals and halogens, and low environmental load.

- Super capacitor are used in the applications that requires rapid charge discharge cycles rather than those which stores compact energies mostly used in automobiles, buses, trains, cranes and elevators, for regenerative braking short-term energy storage, or burst-mode power delivery [2].

Supercapacitor uses electrostatic double layer capacitance and electro chemical pseudo capacitance that gives the total capacitance of the capacitor rather than conventional solid dielectric [3].

In the changing worldwide scenario, energy production and storage, its saving with high efficiency has become a prime focus to the scientific community. The great interest in developing and refining more efficient energy storage devices lead to, the evolution of supercapacitor has matured significantly over the last decade and emerged with the potential to facilitate major advances in energy storage [4]. The continuous effort for energy sustainability, supercapacitors are emerging as devices of prime importance owing to their superior characteristics unmatched by any other charge storage device. The same characteristics have been ruled in various applications such as power electronics, large scale transport systems such as trains and buses, energy storage at intermittent generators including windmills, and smart grid applications. Supercapacitors are also known as ultra-capacitors or electrochemical capacitors; utilize high surface area electrode materials and thin electrolytic dielectrics to achieve capacitances with several orders of magnitude larger than conventional capacitors [5]. In doing so, supercapacitors are able to attain greater energy densities while still maintaining the characteristic high power density of conventional capacitors. Supercapacitor is a typical energy storage device which possesses high specific capacitance, high power density and long cycle life [6]. Supercapacitors can be used in combination with batteries to meet the start-up power, usually high power density.

Conventional capacitors consist of two conducting electrodes separated by an insulating dielectric material. When voltage is applied to a capacitor, opposite charges accumulate on the surfaces of each electrode.

The charges are kept separate by the dielectric, thus producing an electric field that allows the capacitor to store energy.

. Capacitance ‘C’ is defined as the ratio of stored (positive) charge ‘Q’ to the applied voltage ‘V’ i. e,

$$C=\frac{Q}{V} \quad \ldots\ldots\ldots\ldots\ldots\ldots\ldots\ldots\ldots (1.1)$$

In conventional capacitor, C is directly proportional to the surface area ‘A’ of each electrode and inversely proportional to the distance ‘D’ between the electrodes i. e,

$$C = \varepsilon_o \varepsilon_r \frac{A}{D} \quad \ldots\ldots\ldots\ldots\ldots\ldots\ldots\ldots (1.2)$$

The product of the two factors ε_o and ε_r of the equation is a co proportionality constant where ε_o is the dielectric constant (or “permittivity”) of free space and ε_r is the dielectric constant of the insulating material between the electrodes. The two primary attributes of a capacitor are its energy density and power density. The density can be calculated as a quantity per unit mass or per unit volume. The energy E stored in a capacitor is directly proportional to its capacitance:

$$E=\frac{1}{2}CV^2 \quad \ldots\ldots\ldots\ldots\ldots\ldots (1.3)$$

In general, the power P is the energy expended per unit time. To determine P for a capacitor, though, one must consider that capacitors are generally represented as a circuit in series with an external ‘load’ resistance R, as shown in figure 1.2 below.

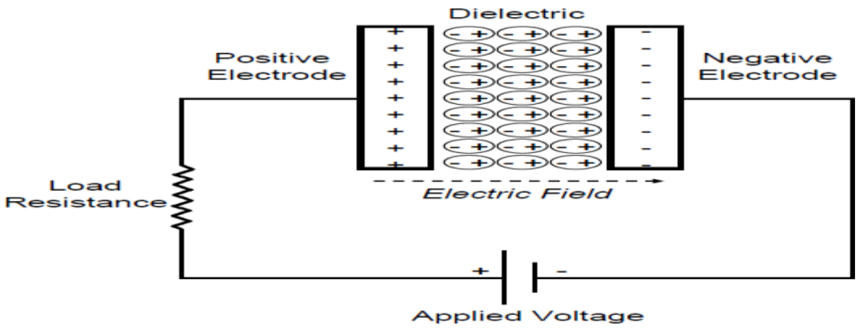

Fig: 1.2 Schematic figure of a conventional capacitor [4]

Conventional capacitors have relatively high power densities, but relatively low energy densities as compared to electrochemical batteries and fuel cells. So a battery can store more total energy than a capacitor, but it cannot deliver it very quickly, that means, its power density is low. Capacitors, on the other hand, store relatively less energy per unit mass or volume, but their power density is usually high [4].

Supercapacitors have the same basic principles as conventional capacitors, but the charge storage mechanism is different from that. Conventional capacitor charge directly in dielectric materials but the supercapacitors use electrolyte ions, which create charge storage in electrical double layers. A subclass of supercapacitors, called pseudo capacitors, exploits yet another mechanism for charge storage via faradaic chemical reactions at the anode. However, electrodes with much higher surface areas ‘A’ and much thinner dielectrics that decrease the distance ‘D’ between the electrodes are used. Thus, from equation 2 and 3, this leads to an increase in both capacitance and energy. In addition, supercapacitors have merits over electrochemical batteries and fuel cells since it has higher power density, shorter charging times, and longer cycle life and self-life [4-6]. Some of the limitations of batteries are also displaced by the supercapacitor, but generally cannot replace them. Rather, they can be used in certain applications where batteries fail and also they can be used as supplements to batteries.

The plot of the power densities of various energy storage devices against their energy densities shows that supercapacitors occupy a region between conventional capacitor and batteries, which is shown in figure 1.3 [4]. Since super capacitors have greater capacitances than conventional capacitors, supercapacitors have to match the energy densities of mid to high-end batteries and fuel cells. Thus, much of the researches give focus on developing improved super capacitors to make their energy densities more comparable to those of batteries.

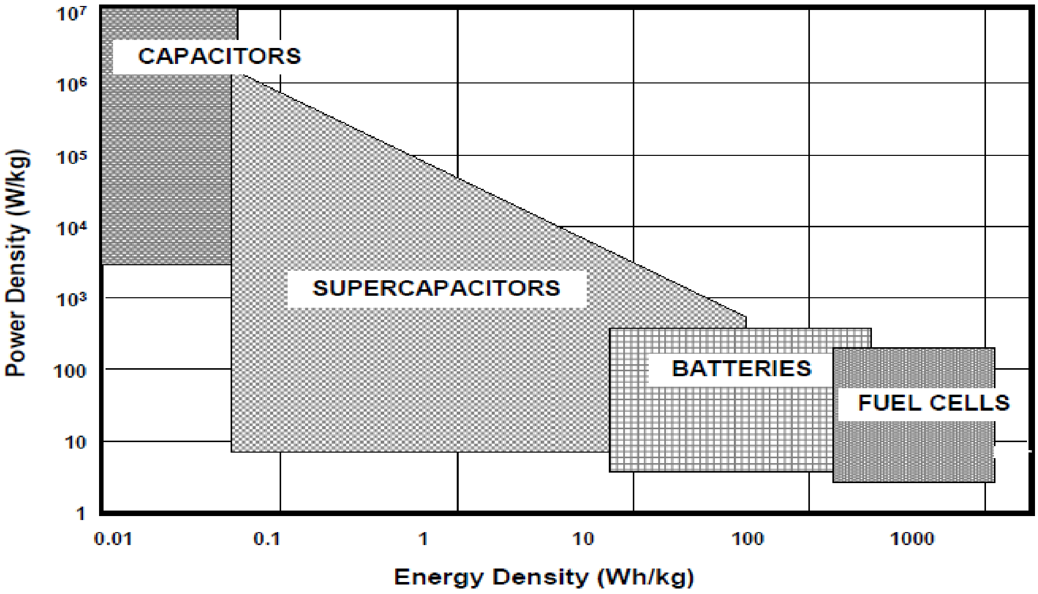

Fig: 1.3 Ragone plot of energy storage devices [4]

1.2 Classification of Supercapacitors

On the basis of current research and findings, supercapacitors can be divided into three general classes: electrochemical double-layer capacitors, pseudo capacitors, and hybrid capacitors [8]. Each class is characterized by its peculiar mechanism for storing charge. i.e. non-faradaic, faradaic and a combination of the two respectively. Faradaic processes, such as oxidation-reduction reactions, involve the transfer of charge between electrode and electrolyte. In non-Faradaic mechanism, there is no any chemical mechanism. Rather, charges are distributed on surfaces by physical processes that do not involve the formation or rupture of chemical bonds [4]. Different types of supercapacitors along with their sub types are presented in Fig: 1.4 among them metal oxide doped polymers type supercapacitor is of interest.

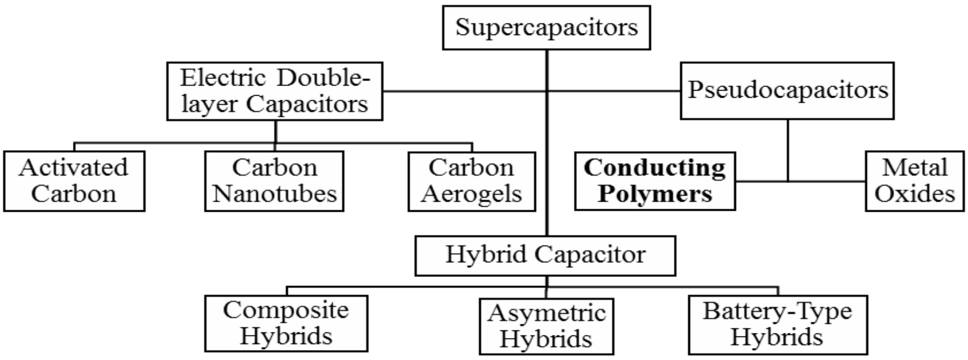

Fig: 1.4 Classification of supercapacitors [6]

1.2.1 Electrostatic double-layer capacitors (EDLCs)

EDLCs uses carbon electrodes or derivatives with much higher electrostatic double-layer capacitance than electrochemical pseudo capacitance, achieving separation of charge in a Helmholtz double at the interface between the surface of a conductive electrode and an electrolyte. The separation of charge is of the order of a few angstroms (0.3–0.8 nm), much smaller than in a conventional capacitor. Electrochemical double layer capacitors (EDLCs) store charge using reversible adsorption/desorption of ions of the electrolyte electrostatically on the surface of the electrode. Carbon materials are most commonly used for EDLCs due to their high specific surface area and low cost. Due to the low cost associated with these capacitors, the commercial market of ECs is highly dominated by EDLCs. The EDLCs consist of two electrodes which immersed in an electrolyte with ion in permeable separator. In this device, the two electrodes are completely isolated electrically such that each electrode-electrolyte interface represents a capacitor [9]. EDLC have high-power capabilities, their energy density is well below that of batteries. The reason is that in contrast to batteries, there are no redox reactions and charge is stored at the surface of the electrode material (i.e. carbon).Thus, the charge can be quickly discharged or charged, but the amount of charge stored at the interface is limited [10].

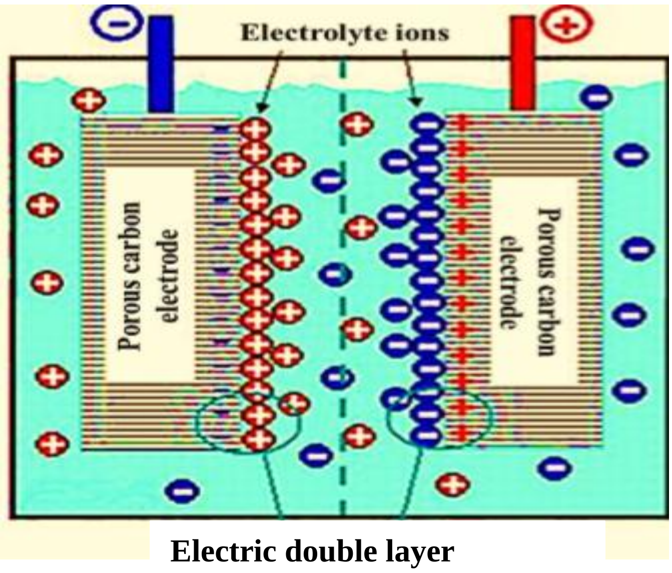

Fig: 1.5 Models of EDLs

1.2.2 Hybrid capacitors

Hybrid capacitors such as the lithium-ion capacitors use electrodes with differing characteristics: one exhibiting mostly electrostatic capacitance and the other mostly electrochemical capacitance. It is the special type of capacitor system in which one battery-type faradaic electrode (as energy source) is connected with the other capacitive electrode (as power source) in the same EC cell, which is called hybrid capacitors'. Hybrid capacitors combine the best features of electric double layer capacitors (EDLCs) and pseudo capacitors together into a unified supercapacitor.

They make use of both physical and chemical charge storage mechanisms together in a single electrode. The main advantage of these hybrid electrodes over the other electrodes is that these electrodes have been able to achieve superior cycling stability comparable to that of EDLCs while retaining the high storage capacity of faradic electrodes [12-13].

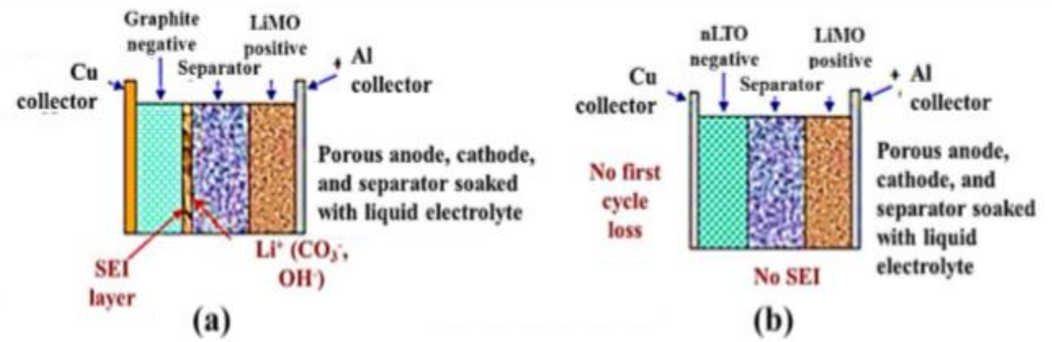

Fig: 1.6 Model of Hybrid capacitors

1.2.3. Pseudo capacitors

Electrochemical pseudo capacitors use metal oxide or conducting polymer electrodes with a high amount of electrochemical pseudo capacitance additional to the double-layer capacitance. Pseudo capacitance is achieved by faradic electron transfer with redox reaction intercalation reactions or electro sorption. In divergence to EDLCs that stores charge electrostatically, pseudo capacitors stores charge faradaically through the charge transfer between electrode and electrolyte. Which is accomplished through electro sorption, reduction-oxidation reactions, and intercalation processes [17, 18, 19]. These

Faradaic processes may allow pseudo capacitors to achieve greater capacitances and energy densities than EDLCs [14, 15, 16]. There are two electrode materials that are used to store charge in pseudo capacitors, conducting polymers and metal oxides. Among the various conducting polymers PANI is of interest.

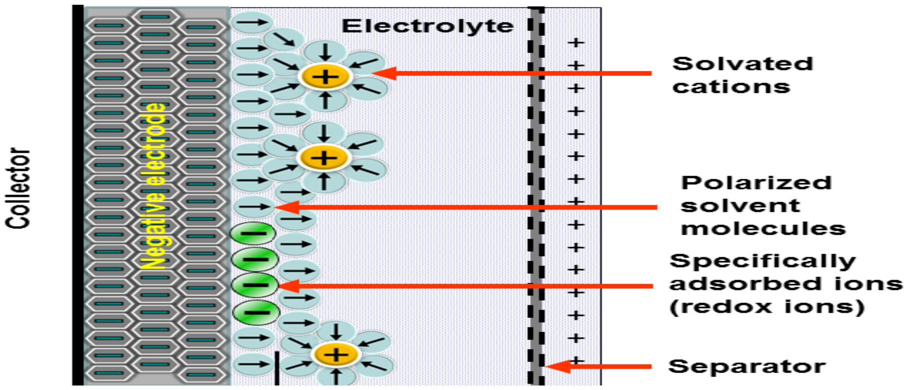

Fig: 1.7 Models of Pseudo capacitor

1.3 Materials for supercapacitor

The super capacitor materials used are polyaniline and Lanthanum oxide.

Polyaniline: Extensive researches are going on in the field of super capacitors as they have wide range of applications such as on computer memory backup, automobiles trains in automobiles, buses, trains, cranes and elevators, where they are used for regenerative braking, short-term energy storage, or burst-mode power delivery. Supercapacitors consist of two electrodes separated by electrolyte here the active surface area of the electrode material is of prime importance. Among various materials here we are concerned with the doping of the transition metal oxides on the conducting polymer polyaniline has become matter of interest for super capacitors applications because it can be polymerized easily and cheap environmental stability, high and controllable conductivity [20, 21, 22] but its defect is that less stable in life cycle and undergoes more swelling and shrinkage effect and poor mechanical property [23]. Transition metal oxides are considered to be best for the application [24 25].The Researchers have diverged in transition metal oxides after the information about the toxic property of ruthenium oxide was known. Aniline monomer has been used for the preparation of the conducting polymer PANI.

The extensive study is going on for polyaniline since last two decades, it was first synthesized by H. Letheby of the College of London Hospital, during anodic oxidation of aniline in sulphuric acid in1826 [26]. PANI was rediscovered in the early 80’s the polymerization of polyaniline can be done by chemical oxidative method, electrochemical oxidative method and aqueous oxidative polymerization method [27].

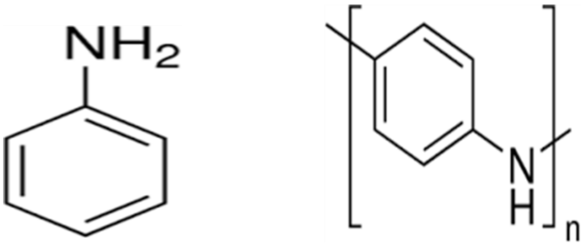

A B

Fig: 1.8 A Aniline B Polyaniline

PANI is the conducting polymer with the extended pie –conjugated system so it is the good applicant for the super capacitors due to high mobility charge carrier [28]. PANI even in undoped or partially doped condition can act as electron donor and carries significant mA of current [29]. As a result PANI doped with Nano metal oxides has its importance in the field. PANI has good possibility, ease of preparation, environmental stability, photoelectric property, cost effectiveness and potential in the field of catalysis, anti-corrosion behavior, biosensors, batteries, electronics, opto-electronics and electronic technology .It can be prepare by chemical electrochemical and by insitue aqueous oxidative polymerization methods. Among these methods later one is the most effective for the preparation of thin films. PANI can be doped with metal oxides in acidic medium, mineral acid dopant can be (hydrochloric, sulfuric, nitric, perchloric, fluoroboric acids) or organic acids (p-toluenesulfonic, benzenesulfonic, p-styrenesulfonic acids), or polymeric acids (polyamic, polyacrylic, polyvinylsulfonic acid) [30]. Beside this various oxidants often reported are sodium or ammonium peroxydisulfate (VI), ammonium peroxydisulfate /ammonium cerium (IV) nitrate mixture, chromate (VI) potassium, ammonium persulphate, ferric chloride and hydrogen peroxide [31].

PANI has three oxidation states Leucoemeraldine,fully reduced form(+1 O.S) Emeraldine, half oxidized form(1/2 O.S) and Pernigraniline, fully oxidized form(0 O.S).The most stable form among this is Emeraldine form [32].

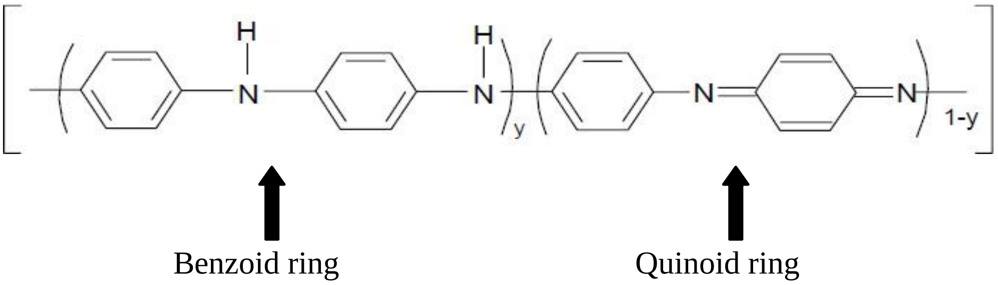

Fig: 1.9 Different form of PANI for y=1 the oxidation state is leucoemeraldine, for y=0 the polymer is in the pernigraniline oxidation state and for y=0.5 the polymer is in the emeraldine oxidation state**.**

These form are inter convertible from each other that can be shown as

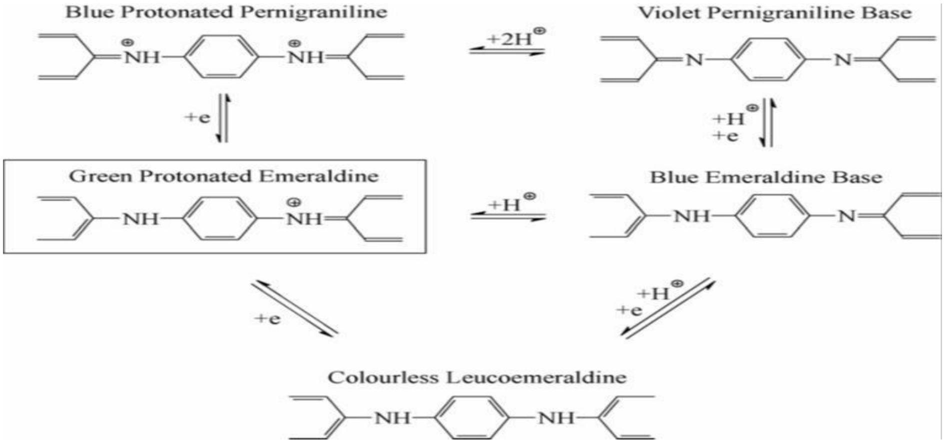

Fig: 1.10 Different inter convertible form of PANI [34]

For the polymerization of the aniline monomer to polyaniline(PANI) the oxidants used are ammonium persulfate $(NH_4)_2S_2O_8$, potassium dichromate ($K_2Cr_2O_7$) ferric chloride ($FeCl_3$), auric chloride ($AuCl_3$), copper nitrate ($Cu(NO_3)_2$), copper chlorate ($Cu(ClO_4)_2$), cerium sulfate ($Ce(SO_4)_2$), potassium ferricyanide ($K_3(Fe(CN)_6$), sodium vanadate ($NaVO_3$), potassium iodate (KIO_3), hydrogen peroxide (H_2O_2), formic acid (HCOOH), acetic acid (CH_3COOH), hydrochloric acid (HCl), sulfuric acid (H_2SO_4), phosphoric acid (H_3PO_4), nitric acid (HNO_3) and some Lewis acids [35].

PANI film is oxidized completely to pernigraniline when oxidant is ammonium per sulfate (APS), but in the presence of organic oxidant PANI film is not completely oxidized to pernigraniline [36]. So in this work APS is preferred. The simple polymerization route and mechanisms are shown below.

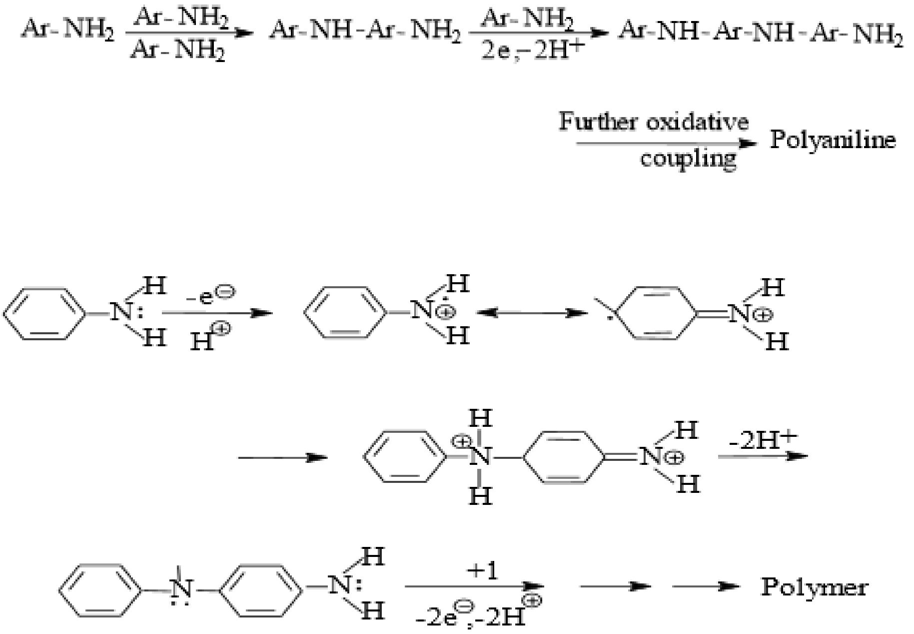

Fig: 1.11 Simple mechanisms for formation of polyaniline [37]

Lanthanum oxide (La_2O_3)

Lanthanum oxide (La_2O_3) is also known as lanthana is an inorganic compound containing the rare earth element lanthanum and oxygen. It is used in some ferroelectric materials, as a component of optical materials, and is a feedstock for certain catalysts. Lanthanum oxide is an odorless, white solid that is insoluble in water, but soluble in dilute acid. Depending on the pH of the compound, different crystal structures can be obtained. La_2O_3 is hygroscopic; under atmosphere, it absorbs moisture over time and converts to lanthanum hydroxide. Lanthanum oxide has p-type semiconducting properties and a band gap of approximately 4.3 eV [38, 39].

Physical properties of La_2O_3

Chemical formula - La_2O_3
Molar mass - 325.809 g/mol
Appearance - White powder, hygroscopic
Density - 6.51 g/cm^3
Melting point - 2,315 °C
Boiling point - 4,200 °C
Solubility - Water insoluble

Its average room temperature resistivity is 10 kΩ.cm that decreases with an increase in temperature, has the lowest lattice energy among the rare earth oxides with very high dielectric constant (ε) = 27. At low temperatures, has an A-M_2O_3 hexagonal crystal structure in which La^{3+} metal atoms are surrounded by a 7 coordinate group of O^{2-}atoms, the oxygen ions are in an octahedral shape around the metal atom and there is one oxygen ion above one of the octahedral faces. On the other hand, at high temperatures lanthanum oxide converts to a C-M_2O_3 cubic crystal structure in which La^{3+} ion is surrounded by six O^{2-} ions in a hexagonal configuration. [41, 42]

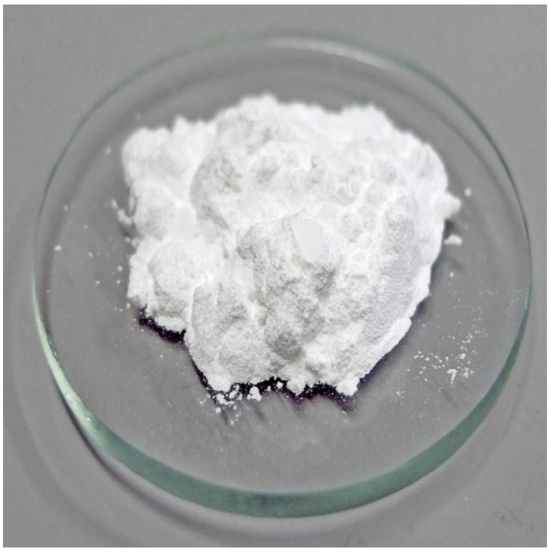

Fig: 1.12 La_2O_3 powder

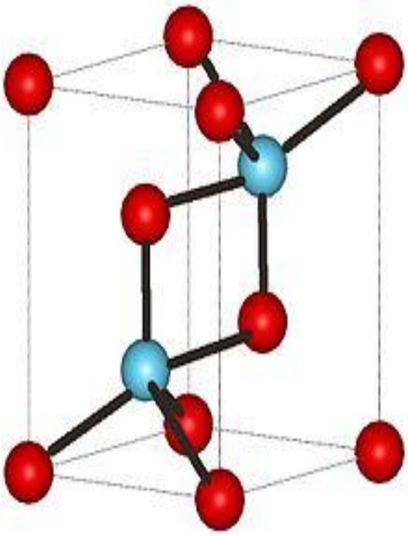

Fig: 1.13 Structure of La_2O_3 [40]

Some common chemical routes to prepare La_2O_3 are as:

a) $2LaCl_3 + 3H_2O \rightarrow La(OH)_3 + 3HCl$

$2La(OH)_3 \rightarrow La_2O_3 + 3H_2O$

b) $LaCl_3 + 3H_2O + 3NH_3 \rightarrow La(OH)_3 + 3NH_4Cl$

$LaCl_3 \cdot 3H_2O \rightarrow La_2O_3$

c) $2La_2S_3 + 3CO_2 \rightarrow 2La_2O_3 + 3CS_2$

$2La_2(SO_4)_3 + \text{heat} \rightarrow 2La_2O_3 + 6SO_3$

Lanthanum oxide is used as an additive to develop certain ferroelectric materials such as La-doped $Bi_4Ti_3O_{12}$ (BLT), in optical materials; usually the optical glasses are doped with La_2O_3 to improve the refractive index of the glasses, density chemical durability, and mechanical strength. When 1:3 reaction mixtures of boron oxide and lanthanum oxide is mixed into a glass composite, the high molecular weight of the lanthanum causes an increase in homogeneity of the melt that leads to a lower melting point [43]. The addition of the La_2O_3 to the glass melt leads to a higher glass transition temperature from 658 °C to 679 °C. Together with oxides of tungsten, tantalum, and thorium, La_2O_3 improves the resistance of the glass to attack by alkali. La_2O_3 is an ingredient for the manufacture of piezoelectric and thermoelectric materials. Automobile exhaust-gas converters also contain La_2O_3 [44]. La_2O_3 is also used in X-ray imaging intensifying screens, phosphors as well as dielectric and conductive ceramics. La_2O_3 has been examined for the oxidative coupling of methane [45]. La_2O_3 films can be deposited by different methods, including chemical vapor disposition, atomic layer deposition, thermal oxidation, sputtering, and spray pyrolysis. Depositions of these films occur in a temperature range of 250–450 °C. Polycrystalline films are formed at 350°C [42]. La_2O_3 tungsten electrodes are replacing thoriated tungsten electrodes in Gas tungsten arc welding (TIG) due to safety concerns with thorium's radioactivity. La_2O_3 has been examined for the oxidative coupling of methane [45].

1.4 OBJECTIVES OF THE STUDY

General objectives:

The general objective of this work was to synthesize La_2O_3 powder and PANI- La_2O_3 Nano composites, characterize them and study their electro chemical behavior.

Specific objectives:

The specific objectives of this research work are:

1. Synthesis of La_2O_3 powder.

2. Synthesis of PANI- La_2O_3 Nano composites.

3. The study of specific capacitance from the CV.

4. The study of the charge discharge capacitance of composite as electrode material.

1.5 LITERATURE REVIEW

This literature survey mainly consist of various researches performed up to 2018 in super capacitors mainly emphasized in metal oxide doped polymer composites especially transition metal oxides. Previously Platinum based electrode catalyst had been used as electrode catalysis but recent researches are focusing on the fabrication of metal oxides and conducting polymer Nano composite on electrode surfaces [46, 47].

For supercapacitors, nanostructured electrode materials have become noteworthy because of their better rate property and capability than traditional materials which is a result of the smaller distance between the electrode and the electrolyte, which favors the transport of ions. Now a days, transition metal oxides, carbon materials and conducting polymers have been widely used as electrode materials with prominent capacitive properties.

Doping of the metal oxides in conducting polymer has been used for enhancing the power density and enlarging the capability of electron accepting and donating during charging and discharging.

At about early 1950's General electric engineers initiated experimenting to design capacitors with the porous carbon electrodes and activated charcoal electrolyte, In 1957 H. Becker got success to form low voltage electrolytic capacitors with porous electrodes [48,49,50].

In 1966 researcher of Standard oil of Ohio (SOHIO) developed electrical energy storage device called capacitor while working on fuel cell designs [51, 52]. in 1970, Donald L. Boos Patented electrochemical capacitors with activated carbon electrode. Nippon Electric Company (NCE) marketed the findings as SUPERCAPICATOR in 1971 to back up the computer memory power [52].

In the period of 1975-1980 Brian Evans Conway worked on ruthenium oxide electro chemical capacitors. Latter in 1991 he lighted about storage mechanism difference between the battery and the supercapacitors [53, 54].

The first supercapacitors with low internal resistance was reported in 1982 for military application by Pinnacle Research institute

David A. Evans developed “Electrolytic-Hybrid Electrochemical Capacitor” by combining the features of electrolytic and electrochemical capacitors [55, 56] in which high dielectric strength of anode from electrolytic capacitors with high capacitance of a pseudo capacitive ruthenium oxide (IV) cathode from electro chemical capacitors [57].

The ruthenium oxide capacitors has good potential and has high specific conductance of 1000 F/g in 1 M H_2SO_4 at room temperature [58] but it was toxic so in replacement of it researches turned towards the other transition metal oxide doped in the polymers because the transition metal oxide are potential materials for supercapacitor applications due to their pseudo capacitive behavior. Current researches focuses on metal oxide like: NiO, MnO_2, FeO, TiO_2, SnO_2, IrO_2, V_2O_5, La_2O_3, MoO *etc.* because their doping on conducting polymer enlighten the researchers towards the synthesis of unique material for redox supercapacitor electrode material.

Bigg*et al*. made polymers conducting with the help of fillers [59]. Clark *et al.* increased the electrical conductivity of these systems by several orders of magnitude by advances in the synthesis of organic conducting polymer systems in the last decade [60].

In 1968, it was shown that polyaniline could be transformed to a conducting form by oxidation or protonation by Surville, *et al*. [61].

Huang*et al.* rediscovered polyaniline as an organic conducting polymer in 1986 [36], and since that time extensive research has been done to explore its potential applications in electronics and energy storage [61-63].

Some literatures have reported the modified electrode (composites) of carbon based material with conducting polymers.Song *et al.*prepared Polyaniline/nafion /hydrous RuO_2 composite by chemical method and obtained the specific capacitance value of 475 F g^{-1} [64].

Yang *et al.* demonstrated a novel kind of PANI-CNTs composite, which exhibited a specific capacitance value of 163 F g^{-1} at a current density of 1 A g^{-1}[65]. The other type of in situ polymerization composite of polyaniline/multi-walled carbon nanotube showed the highest specific capacitance value of about 560 F g^{-1} by Zhou *et al.* [66].

Chen *et al.* have reported the specific capacitance value of 180 F g^{-1} for polyaniline/porous carbon composite electrode materials [58]. Recently, graphene oxide/PANI composite has been evaluated by Wang *et al.*, the reported specific capacitance value being about 531 Fg^{-1} [67].

Mujawar *et al.* conducted electro polymerization of polyaniline/titanium oxide nano composite and found specific capacitance value about 740 Fg^{-1} [68].

Chen *et al.* found that electrochemically synthesized MnO_2/PANI composite electrode exhibited a specific capacitance value of 80 F g^{-1} and it has stable columbic efficiency of about 98 % up to 1000 cycle [69]. Patil*et al.* PANI/TiO_2 reported maximum specific capacitance value 248-898 F g^{-1} at different scan rates, whereas nano-composite was formed between polyaniline [70]. Yang *et al.* were observed that PANI/Graphene composites was found to have improved cycling stability and increase of specific capacitance value from 147 Fg^{-1} to 210 Fg^{-1} [71].

Kalako dimi *et al* in 2004 prepared Indium oxide electrode for high performance electrode materials for redox super capacitors and the specific conductance found to be 190 F/g at the scan rate of 10 mV/s [72].

Chen.Ye *et al* synthesized lanthanum oxide doped MnO electrodes for super capacitors application and found charge discharge capacity of 156.15F/g and charge diascharrge cycle was increased by 19.5% than that of pure MnO electrode [73].

Rahul R.S. Aalunkhe *et al* in 2014 Synthesis of reduced Graphene Oxides with uniformly coated Polyaniline for Supercapacitor application and got a high specific capacitance of 286 F g^{-1} and high cycle reversibility of 94 % after 2000 cycles [74].

Zihang Huang *et al* Synthesized PANI/La_2O_3 and PANI/Sm_2O_3 by insitue polymerization in presence of Sulpho Salicyclic acid and only studied about the thermal stability and found that thermal stability was more than the pure PANI [75].

Yi CaO *et al* in 2015 synthesized the Sr-doped Lanthanum Nickelate Nanofibers for high energy density supercapacitors and specific conductance was found to be 719 F/g Energy density 81.4 Wh.kg^{-1},Power density of 500 Wh.kg-^{1} .with excellent cycling life [76].

Yi CaO *et al* in 2015 synthesized Lanthanum Manganese fibers doped with Sr and Cu by electrospinning nanofibers and specific capacitance was found to be 464.5 F/g current density of 2A/g and energy density of 64.5 Wh.kg^{-1}[77].

Jingbo LV *et al* in 2016 synthesized Strontium Lanthanum Manganite in Manganesedioxide composite by hydrothermal method and capacitance was found to be 437.2F/g much better than pure PANI [78].

Nandarajan Arjun *et al* in 2017 explored lanthanum based perovskites and their complementary electrodes for the super capacitor application and found highest specific capacitance of 106.58F/g for $LaNiO_3$ electrodes in 3 M LiOH electrolyte [79].

Rajesh Rajagobal *et al* in 20018 prepared La/Ce mixed MnO_2 Nano structure for the super capacitor application and specific capacitance of 1165 F/g was detected [80].

Anuj Kumar *et al* in 2019 prepared lanthanum molybdenum oxide using different calcination temperature, lanthanum molybdenum oxide prepared at the temperature of 500 ^{o}C obtained the maximum specific conductance of 772.18 Fg^{-1} [81].

CHAPTER-2: EXPERIMENTAL METHODS

2.1 Materials

The chemical used, EDTA, Sulphuric acid, Ammonium persulphate, were purchased from Merk chemicals India. Lanthanum nitrate **La $(NO_3)_3.6H_2O$** (MW: 433.02) was purchased from Fisher scientific India. Aniline, oxalic acid, acetone were used from Central department of chemistry Nepal. PVDF binder, solvent NMP, Ni-form, and carbon black powder were purchased from Xian Top New Energy Technology Co. Ltd. China. All the required solutions were prepared in Physical chemistry thesis laboratory of central department of chemistry. The instruments used were taken from the CDC laboratory. The distilled water required was brought from KIPU Kirtipur, Nayabazar.

2.2 Methods

2.2.1 Synthesis of lanthanum oxide powder

By precipitation method: 25 mL of 1M lanthanum nitrate was dissolved in 25 mL of EDTA solution then, to the mixture a solution of 10% oxalic acid was added under constant stirring until the pH of 3-4 after complete precipitation white ppt of lanthanum oxide was obtained which was separated by filtration and washed with distilled water several times and dried at 110 ^oC for about 12 hrs, Finally calcined at 800 ^oC for three hours [82].

2.2.2 Purification of aniline

Purification of aniline was done by constructing the distillation flask. Aniline was taken in RB flask and subjected for distillation as shown in figure below. The boiling point of aniline is 140 ^oC. Double distillation was performed to enhance the purity of the aniline then aniline was subjected for the polymerization.

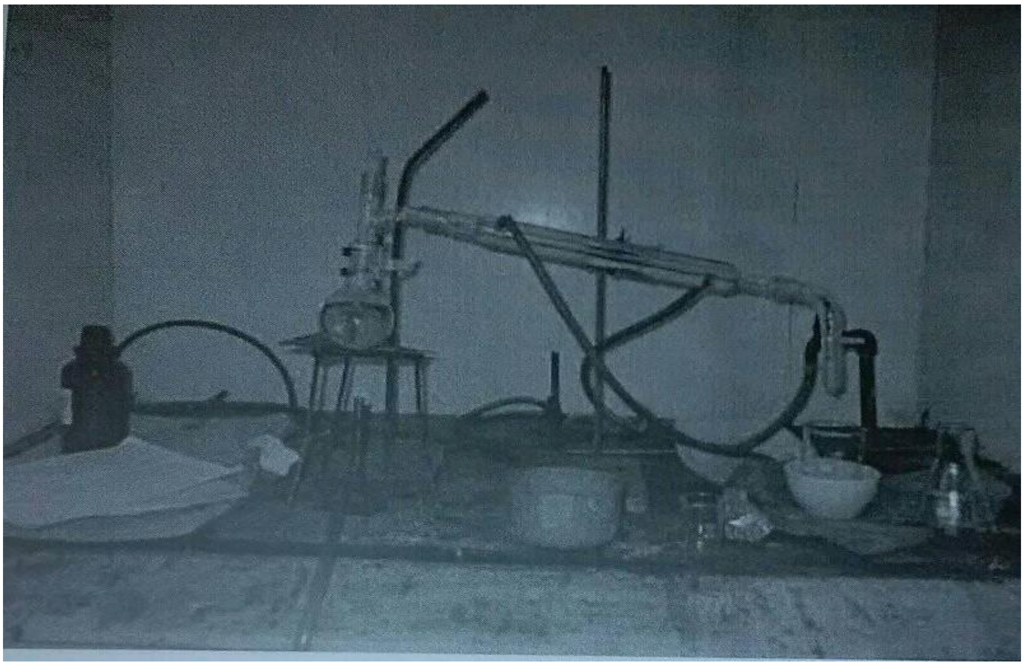

Fig: 2.1 Distillation of Aniline

2.2.3 Polymerization of Aniline

Among several methods of polymerization of aniline the most global method is considered to be an oxidative polymerization method, which involves the doping and polymerization together. It can be chemical or electrochemical method. Here chemical oxidative method was used for which the following solutions were prepared.

1. 100 mL of 0.22 M of aniline in 1 M H_2SO_4.
2. 100 mL of 0.24 M of APS in 1 M H_2SO_4.

50 mL of APS solution was taken in the burette and 50 mL aniline in the beaker. The APS solution was added to the beaker (about 3 drops/sec) with continuous stirring. After the completion of the addition it was continuously stirred for 6 hrs and left overnight to polymerize. The dark green PANI precipitation was obtained which was transformed to the whatman paper for the filtration, it was washed several time with distilled water and acetone until the filtrate turned colorless the residue was dried for 12 hrs in air and 24 hrs in oven at temperature of 70-75 ^{o}C. Thus obtained sample was kept in air tight borosil.

2.2.4 Preparation of PANI-La_2O_3 Nano composites by aqueous oxidative polymerization method

PANI-La_2O_3 Nano composite was prepared in situ by aqueous oxidative polymerization method. Different proportions of La_2O_3 (0.1, 0.2, 0.3, 0.5 g) was added to 50 mL of 0.22 M of aniline in 1 M H_2SO_4 in beaker and 50 ml of APS solution taken in the burette was added to it (about 3drops/sec) with continuous stirring. After the completion of the addition it was continuously stirred for 6 hrs and left overnight to polymerize. The precipitation of PANI-La_2O_3 was obtained which was transformed to the whatman paper for the filtration, it was washed several time with distilled water and acetone until the filtrate turned colorless the residue was dried for 12 hrs in air and 24 hrs in oven at temperature of 70-75 ^{o}C .Thus obtained sample was kept in air tight borosil bottle.

2.3 Characterization and Measurements

The sample characterizations of were carried out by using Fourier transform infrared spectroscopy (FTIR), X-ray diffraction (XRD), UV-Visible Spectroscopy, Scanning electron microscopy (SEM), Energy dispersive X-ray spectroscopy (EDX), Cyclic voltammetry (CV) and Galvanostatic charge-discharge (GCD).

2.3.1 Fourier transforms infrared spectroscopy (FTIR)

FTIR helps to find the functional group present in the prepared active materials the nature of bonding in the materials. The IR absorption spectra were recorded for La_2O_3, PANI and prepared composite samples with varying amount of the oxide in the spectral range of 4000-400 cm^{-1} using an IR Prestige-21 FTIR spectrometer (SHIMADZU) in Central Department of Chemistry, Kathmandu, Nepal.

2.3.2 X-ray diffraction (XRD)

X-ray diffraction (XRD) is a non-destructive method for the analysis of the structure, purity, of the crystalline materials, also helps to know the crystal structure and spacing between the crystal lattice and is based on the Bragg's law ($n\lambda=2d\sin\theta$). Bragg's law relates the wavelength of the incident x-ray, angle of incidence and spacing between the crystal lattice. The crystal structure of La_2O_3, PANI and La_2O_3-PANI composite samples with varying amount of the oxide were investigated by powder X-ray diffraction (XRD) measurements on a BRUKER diffractometer (CuKα radiation source, λ= 0.15406 nm) in the range of 2θ = 10-90° in Nepal Academy of Science and Technology (NAST), Khumaltar, Lalitpur, Nepal. The average particles size was calculated by using Debye-Scherer's equation. This is given by

$$B= \frac{K\,\lambda}{\beta cos\theta} \ldots\ldots\ldots\ldots\ldots\ldots (2.1)$$

Where, B is the average crystallite size, λ is x-ray wave length of CuKα radiation (0,154 nm) θ is the diffraction angle (in radian) and β the full width of half maximum of the peak the value of K=0.9

2.3.3 UV-Visible Spectroscopy

UV-Visible Spectroscopy is used in analytical chemistry for the quantitative analysis for detection of different analytes. About 1 mg of active materials were dissolved in 10 mL of NMP solvent at room temperature to get solutions of La_2O_3, PANI and La_2O_3-PANI composite samples with varying amount of the oxide. The UV-Visible spectra of these solutions were recorded by using SPECORD 200 PLUS spectrophotometer, using NMP solvent as reference, in range 800–300 nm in Central Department of Chemistry, Tribhuvan University, Kirtipur, Nepal. The bandgap energy can be calculated by using the Tauc equation:

$$(\alpha h\nu)^n = A(h\nu-Eg) \ldots\ldots\ldots\ldots\ldots\ldots\ldots\ldots\ldots\ldots (2.2)$$

Where, α = absorption coefficient, h= Planck constant, ν = frequency, A denotes a constant and the value of n depends upon whether the transition is direct or indirect.

2.3.4 Scanning Electron Microscopy (SEM)

SEM creates the surface image with the help of the focused electron beam, normally with the energies of 1-30 KeV, from the source on the on the surface and detects the scattered electrons from the surfaces. The image so obtained provides the topographical, morphological, compositional and crystallographic informations. The surface morphology of prepared samples was examined by analyzing the Inspect TM S50 scanning electron microscope, equipped with an Oxford energy dispersive X-ray spectroscopy (EDS) in the Institute of Metal Research, Shenyang, China.

2.3.5 Energy dispersive X-ray (EDX)

EDX is x-ray based technique used for the identification of the elemental composition present in the sample. The EDX spectrum shows the peaks correspond to the elements present i.e. it helps to know about the elements present in the samples. Elemental distribution on surface was analyzed by using oxford energy dispersive spectroscopy (EDS).

2.3.6 Electrochemical Characterizations

The electrochemical characterization of synthesized active materials helps to calculate the various parameters such as specific capacitance, energy density, power density, stability and helps to identify the pseudo capacitive behavior. The electrochemical measurements were performed by conventional three-electrode system, saturated calomel electrode as reference electrode and platinum as counter electrode and working electrode of synthesized materials, using potentiostat/galvanostat model HA-151, HOKUTO DENKO made in Japan and LabVIEW software present in Central department of chemistry T.U Kritipur.

2.3.6.1 Preparation of electrode

The working electrode was prepared by coating the active materials into nickel mesh of 0.5 cm × 0.5 cm dimensions. 80 wt.% of active materials was mixed with 10 wt.% of PVDF binder and 10 wt.% of carbon black in a watch glass and grounded using spatula.

Few drops of NMP were poured and again grounded to produce slurry which was then sonicated and spread onto nickel form and pressed hardly with spatula on both sides. Then, it was allowed to dry in oven for 14 hours at around 60^{o}C**.**

i. PANI

ii PANI-La_2O_3 0.1 (S1)

iii. PANI-La_2O_3 0.2 (S2)

iv. PANI-La_2O_3 0.3 (S3)

v. PANI-La_2O_3 0.5 (S4)

Fig: 2.2 Fabrication of electrodes

2.3.6.2 Cyclic Voltammetry (CV)

CV is an electrochemical technique used to measure the current in electro chemical cells by applying the known voltages, based on the Nernst equation. During cycling the potential of the working electrodes is altered and the resulting current is recorded. It provides the information of the electrochemical cells such as capacitance, cycle life, and potential window.

The curves anodic and cathodic record the peaks which is the important parameter. Capacitance can be calculated using CV with the help of following formula.

Capacitance (C) = $\frac{\text{Average Current}}{\text{Scan Rate}}$ …………….. (2.3)

Capacitance (C) = $\frac{Integrated\ area\ of\ Cv\ curve}{2\ \times Potential\ Window\ \times Scan\ Rate}$ . ..……….. (2.4)

Specific Capacitance (SC) = $\frac{Capacitance}{Weight\ of\ Active\ Materials}$……….. (2.5)

CV of the prepared active materials was plotted by using HOKUTO DENKO HA-151 Potentiostat/Galvanostat controlled by Polarization software interfaced with IBM computer.

2.3.6.3 Galvanostatic Charge Discharge (GCD)

GCD is the measure of the charging and discharging current of the prepared active materials, helps to study about the specific capacitance, energy density, power density by the following relations:

Specific Capacitance (SP) = $\frac{(I\times\Delta t)}{(\Delta V\times m)}$ …………………. (2.6)

Where,

I = Charge discharge current

Δt = Discharge time,

ΔV = Voltage difference or potential window

m = mass of the active composite material

Energy Density (E) expresses how much energy a device can store, while power density (P) shows energy spent per unit time. Energy density and power density were calculated by using following formula

E = $\frac{SP\times\ \Delta V^2}{8\ \times 3.6}$ ………… (2.7)

And

P = $\frac{3600\times E}{\Delta t}$ …………… (2.8)

Where unit of E is Watt-hour/kg and P is Watt/kg

GCD was performed by using HOKUTO DENKO HA-151 Potentiostat /Galvanostat controlled by 2ch-Monitor software interfaced with IBM computer in central department of chemistry, Kirtipur, Nepal.

CHAPTER-3: RESULTS AND DISCUSSION

All the prepared samples were subjected to FTIR, UV, X-ray, SEM and EDX. The electrochemical characterization was carried by cyclic voltammetry (CV) and Galvanic charge discharge (GCD).

3.1 Fourier Transform Infrared Spectroscopy (FTIR) Analysis

The FTIR analysis reports are presented as:

3.1.1 FTIR analysis of lanthanum oxide.

FTIR spectra of lanthanum oxide, in the range of 4000-400 cm-^{1} is shown in Figure 3.1.

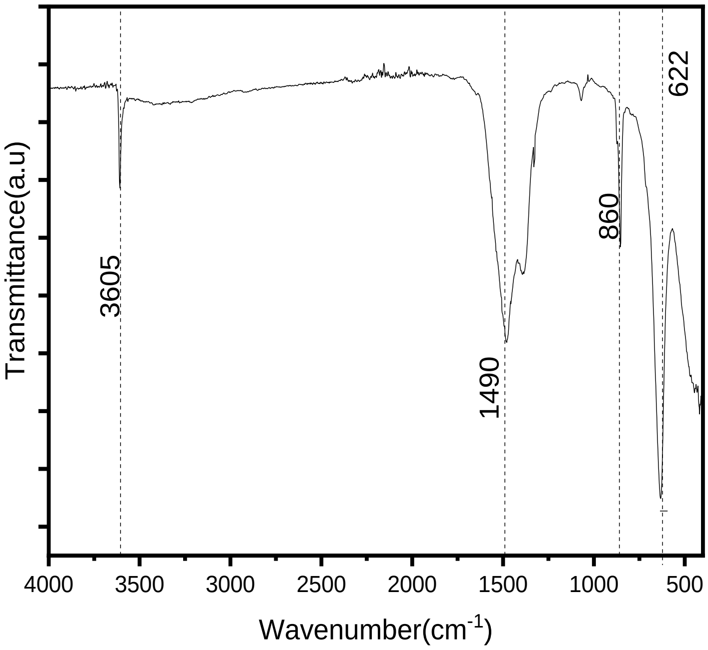

Fig : 3.1 FTIR of Lanthanum oxide

The synthesized La_2O_3 nanocrystals have characteristics peak at 622 cm^{-1} correspond to the vibration band of La-O. The peaks at 1490 and 3605 cm^{-1} is due the O-H stretching of water.

3.1.2 FTIR analysis of PANI

FTIR spectra of PANI, in the range of 400-4000 cm^{-1} is shown in Figure 3.2.

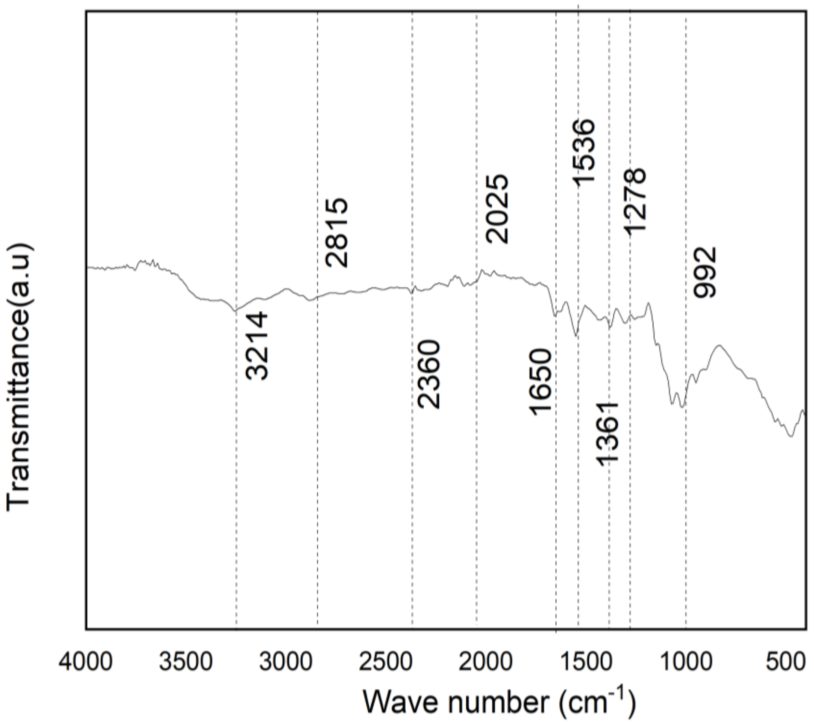

Fig: 3.2 FTIR spectra of PANI

The FTIR spectrum of PANI shows adsorption band at 1650 cm^{-1} due to C= N stretching vibration of quinoid ring. The bands at 1536 and 1361 cm^{-1} are characteristics to C=C stretching vibration of qunoid ring and benzenoid ring respectively. The bands at 3214 cm^{-1} is due to the N-H stretching of aromatic amine, The band at about 1278, and 1363 cm^{-1} is assigned to the C–N bond vibrations.The band at 2815 cm^{-1} due to aromatic C-H stretching. The band at 992 cm^{-1} is due to be quinoid ring-NH^{+} - benzoid ring stretching vibrations which is characteristics band for emeraldine salt being attributed to the doping of PANI with H^{+} [83,84].The above bands indicate the formation of conductive emeraldine salt form.

3.1.3 FTIR analysis of sample composites

FTIR spectra of the sample composites, in the range of 4000-400 cm^{-1} is shown in Figure 3.3.

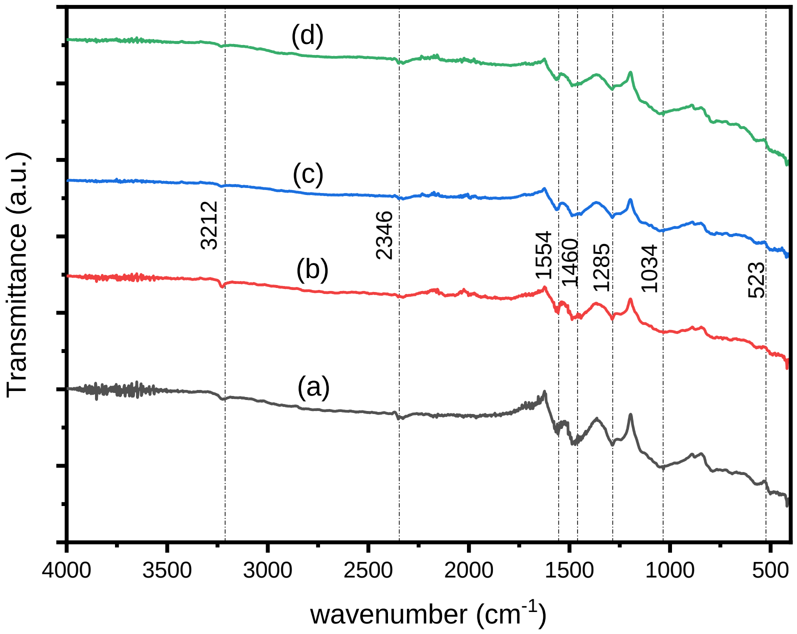

Fig: 3.3 FTIR spectra of the sample composites (a) PANI-La_2O_3 0.1 (b) PANI-La_2O_3 0.2 (c) PANI-La_2O_3 0.3 (d) PANI-La_2O_3 0.5

The similar absorption bands of PANI and La_2O_3 were observed in PANI-La_2O_3 composites with slight shift. This is due to an interaction between PANI chains and La_2O_3 nanoparticles. The reduction in the intensity of these PANI characteristic peaks in PANI- La_2O_3 indicates successful transformation of the PANI molecule to PANI- La_2O_3 nanocomposite.

3.2 X-ray Diffraction (XRD) Analysis.

Figure 3.4 and Fig. 3.5 show XRD patterns of lanthanum oxide and its composites. The spectra suggest the crystalline structure of the lanthanum oxide. The peaks centered at about 2θ values of 28°, 29°, 31°, 39° 49° and58° which are corresponding to face-centered cube structure of magnetite nanoparticles marked with the indices 001, 002, 102, 103, and 201 respectively given in JCPDS file no 020105 [85].

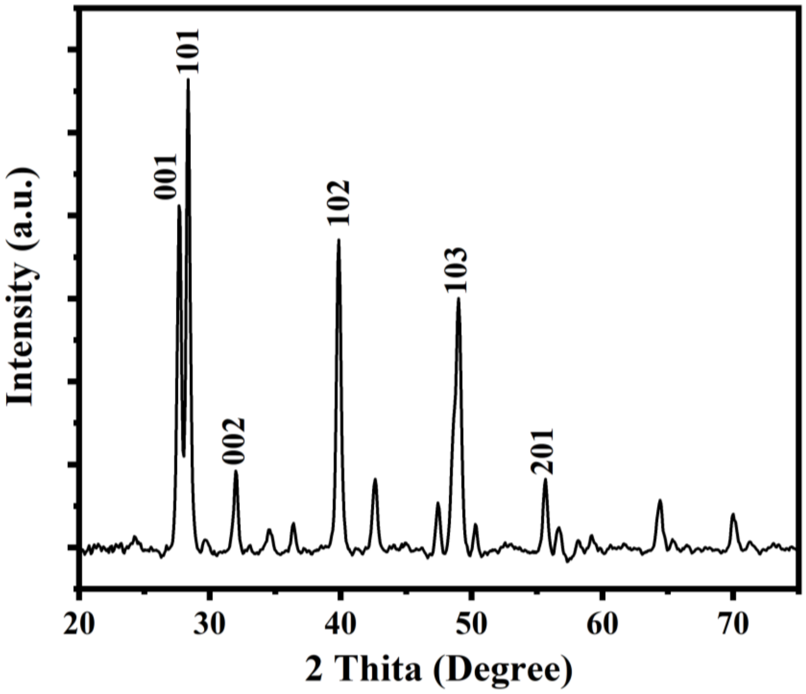

Fig: 3.4 Shows XRD pattern of the lanthanum oxide

It shows that the La2O3 with high purity obtained and the pattern matches with La_2O_3 with hexagonal structure the sharp diffraction peak the sample indicated that well crystallized lanthanum oxide crystals can be prepared under current synthetic procedure. The broadening of the peaks indicated that the particles were of nanometer scale. Average size of the particles was estimated from Scherrer equation, average particles size of the particles was 19.47 nm

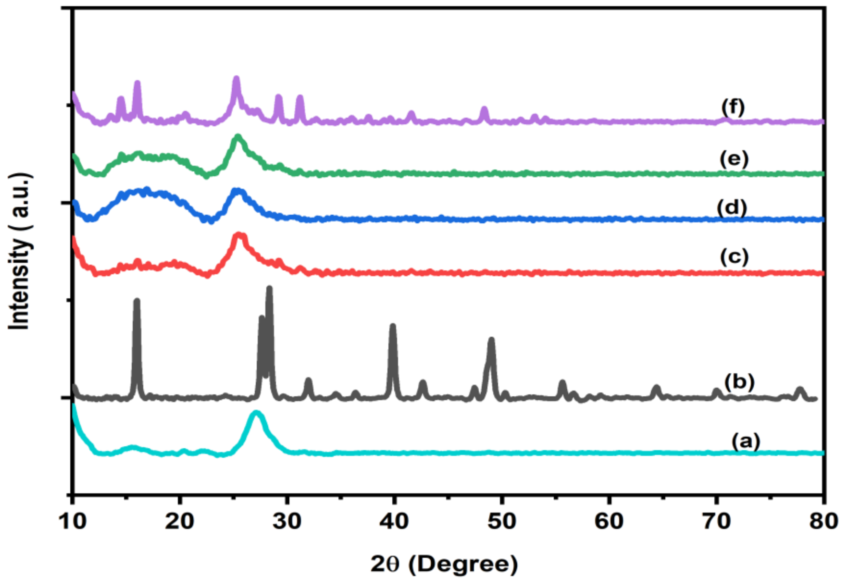

Fig: 3.5 XRD pattern of (a) PANI (b) La_2O_3 (c) PANI-La_2O_3-0.1 (d) PANI-La_2O_3-0.2 (e) PANI-La_2O_3-0.3 (f) PANI-La_2O_3-0.5.

The XRD curve of PANI shows that PANI has partly crystalline structure and two small peaks with one broad characteristics are observed at 2θ values 15.12° and 19.79°, 25.91° respectively, agreed with JCPDS file no. 72-0634. The average crystallite size of polyaniline was calculated as 8.45 nm. The XRD spectra of PANI-La_2O_3 nanocomposites exhibited a diffraction pattern constituted by a mixture of PANI and La_2O_3 peaks. In PANI- La_2O_3 composite there is reduced peaks at about 25.91°shows the presence of PANI. PANI diffraction peak intensities is reduced in the nanocomposite, suggest that PANI is present in the noncrystalline state. Observing the characteristic peaks of La_2O_3 in composite and broadening and weakening the intensity of La_2O_3 peaks suggest that reduction in the crystallinity of La_2O_3 in the nanocomposite. All these observations shows, La_2O_3 was doped with PANI and PANI- La_2O_3 nanocomposite was formed successfully. This reduction of crystallinity of La_2O_3 and improved amorphous phase of PANI is certainly beneficial for electrochemical performance by improving the surface area, more activation sites and shortened charge transport length for the electrochemical process.

3.3 UV-Visible Spectral Analysis

UV spectra of PANI, La_2O_3, different samples of PANI-La_2O_3 corresponding Tauc plot are shown in the Figure 3.6:

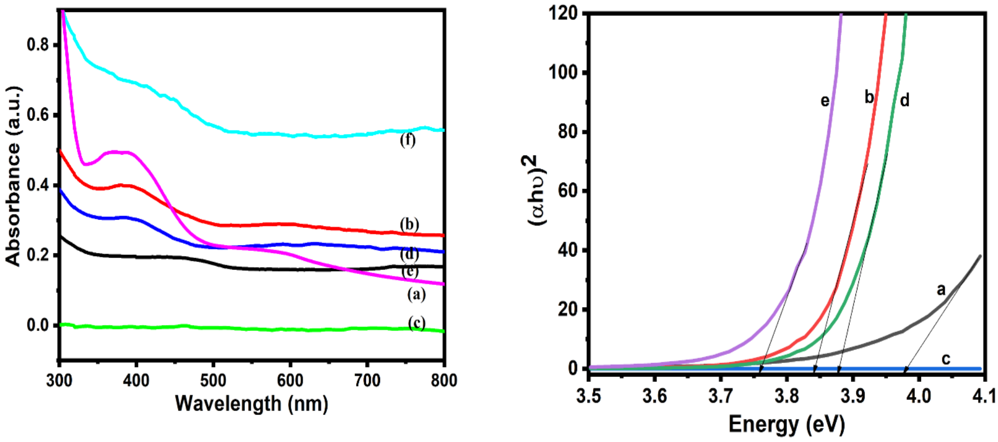

Fig: 3.6 UV spectra of (a) PANI (b) La_2O_3 (c) PANI-La_2O_3-0.1 (d) PANI-La_2O_3-0.2 (e) PANI-La_2O_3-0.3 (f) PANI-La_2O_3-0.5 and corresponding Tauc plot.

UV-Visible absorption spectra for La_2O_3 showed a strong absorption peak at 427 nm which is a characteristics peak for La_2O_3 nanoparticles. Two absorption bands curves was seen for PANI first at 370 nm and second at 600 nm. The first band was of π-π* transition and the next were associated with the transition of benzenoid rings into quinoid rings (π–polaron transition) [61]. In composites, these absorption bands shifted to a lower wavelength, showing interactions between PANI and La_2O_3 in composites. The band gaps energy for PANI, La_2O_3, PANI-La_2O_3-0.1, PANI-La_2O_3-0.2, PANI-La_2O_3-0.3 and PANI-La_2O_3-0.5 are 4, 3.85, 3.99, 3.75, 3.95, and 3.96 respectively. It shows that when band gap decreases electron transfer increases, hence the specific capacitance also increases, so only at the appropriate combination of PANI and oxide the high specific capacitance is observed.

3.4 Scanning Electron Microscopy (SEM) Analysis

The SEM image of pure PANI and La_20_3 under the magnification of X10,000 is shown in Figure 4.4.1(a) and (b) respectively. Figure 4.4.1(a) reveals the irregular nanofiber form of PANI. The PANI nanofibers aggregate structure is observed. Fig 4.4.1 (b) reveals that La_20_3 is present in the Nano sheet form. Figures 4.4.1 (c) (d) (e) (f) illustrate the morphology of PANi-La_20_3 nanocomposites under the magnification of X10,000 revealing a uniform morphology of different composites.

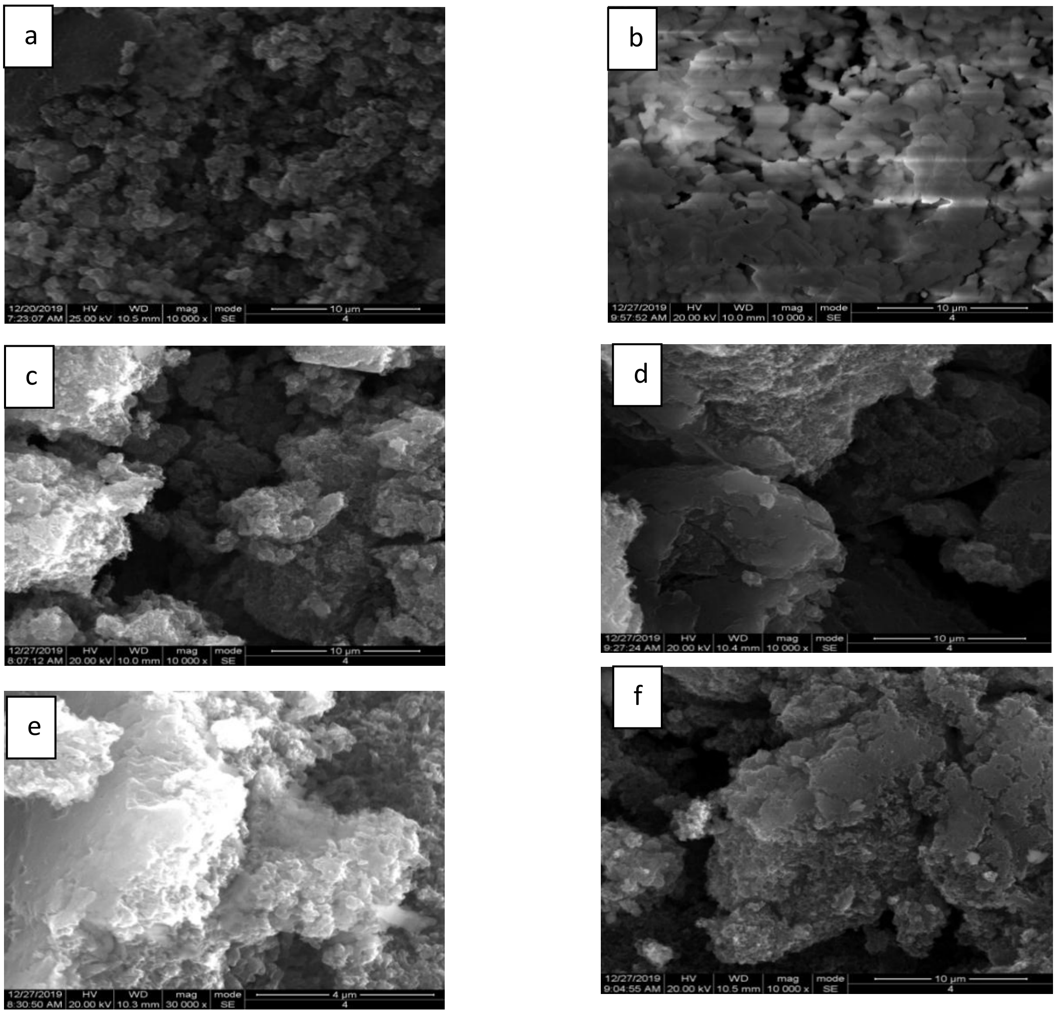

Fig: 3.7 SEM images of different samples (a) PANI (b) La_20_3 (c) PANI-La_2O_3-0.1 (d) PANI-La_2O_3-0.2 (e) PANI-La_2O_3-0.3 (f) PANI-La_2O_3-0.5

The Figure 4.4.1 (d) shows the more uniform combination of both lanthanum oxide and PANI, It reveals that among the prepared electrodes it must give the better performance.

3.5 Energy Dispersive X-ray (EDX) Analysis

The presence of nanoparticles in the nanocomposites was confirmed by EDX analysis. The EDX pattern of PANI shows in Figure 3.8 (a) consists of strong peaks corresponding to Carbon, Oxygen and Nitrogen which confirms PANI formation.

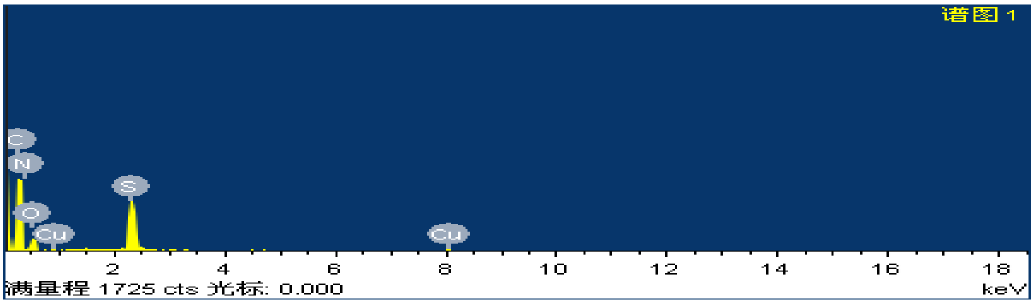

(a)

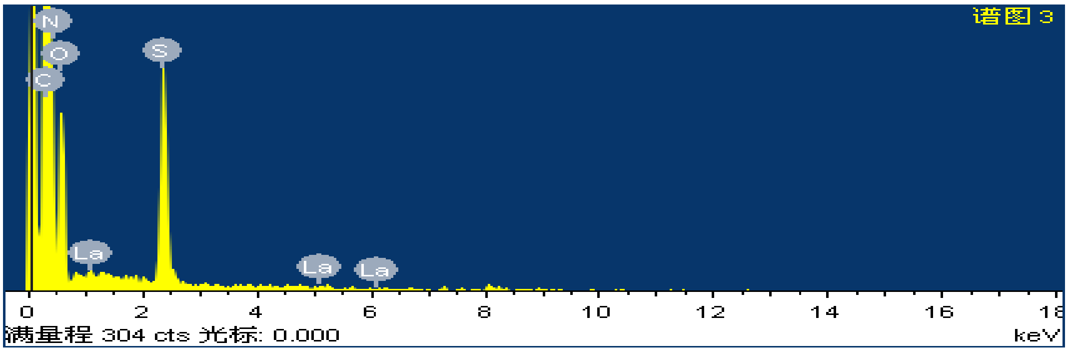

(b)

The EDX patterns of lanthanum oxide in the Fig. 3.8 (b) shows strong peaks corresponding to lanthanum and oxygen which conforms formation of lanthanum oxide.

The EDX patterns of PANI-La_2O_3 composite are shown in Fig. 3.8 (c), (d), (e) and (f) the presence of lanthanum oxide and PANI indicates the successful preparation of PANI-La_2O_3 composites.

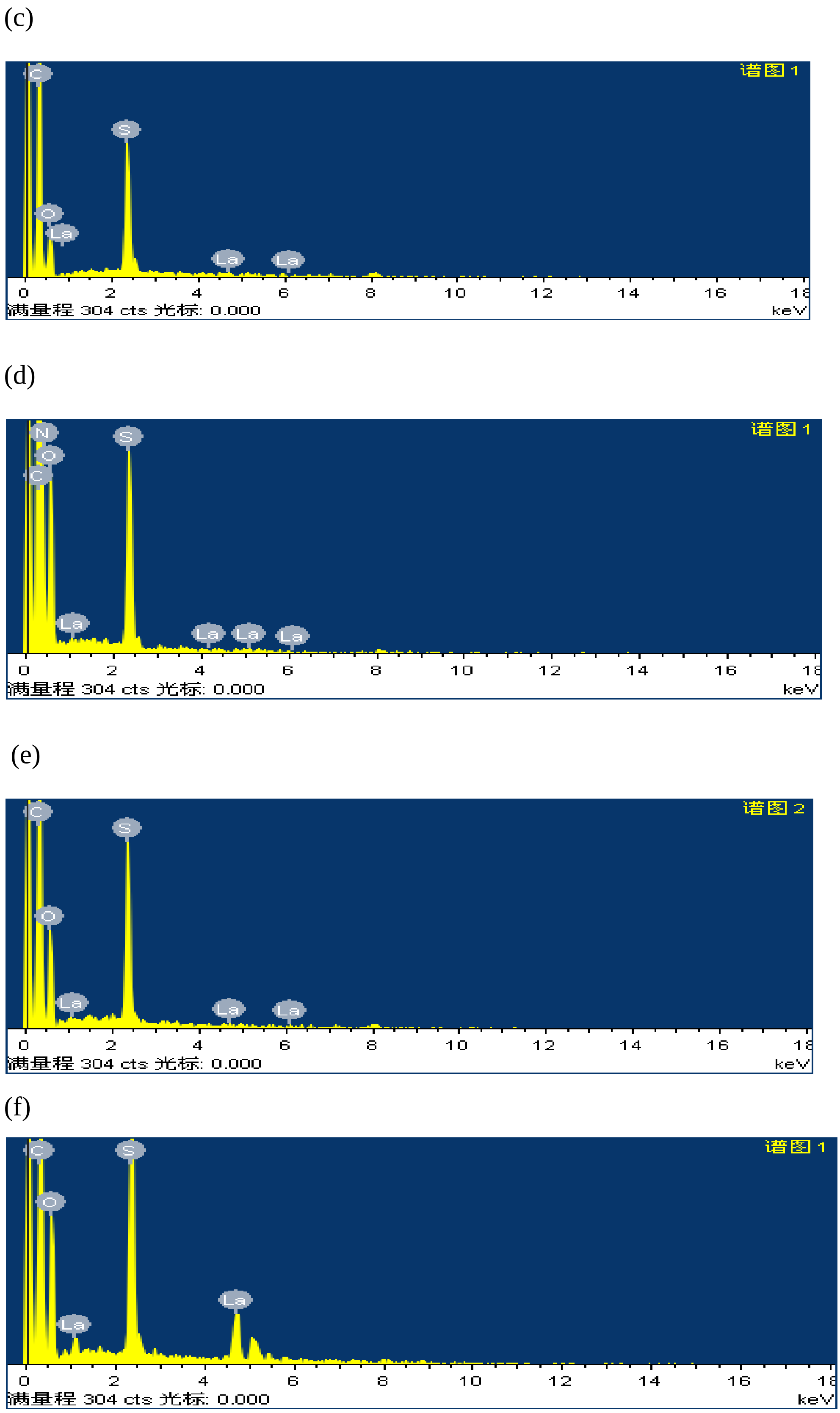

Fig: 3.8 EDX patterns of different samples (a) PANI (b) La_20_3 (c) PANI-La_2O_3-0.1 (d) PANI-La_2O_3-0.2 (e) PANI-La_2O_3-0.3 (f) PANI-La_2O_3-0.5.

3.6 Electrochemical Analysis

The electrochemical analysis of active materials was performed to mount their better application for electrochemical capacitors as electrode materials. The specific capacitance of PANI, Lanthanum oxide doped in PANI with different concentration of oxides were examined by Cyclic Voltammetry and Galvano static Charge/Discharge measurements by applying the potential range of -0.2 to 1.0V. The three-electrode system with 1M H_2SO_4 electrolyte was used for this measurement. [86]

3.6.1 Cyclic Voltammetry (CV)

Figure 3.9 shows the CV of the prepared active materials, PANI, La_2O_3, PANI-La_2O_3 samples, with the scan rate of 10mV/s. The mass of the active material on the surface of electrode for 10 µm depth over which redox reaction occurs was found to be 0.2 mg. The potential range was within -0.2 V to 1V i.e. the potential window of 1.2 V was applied.

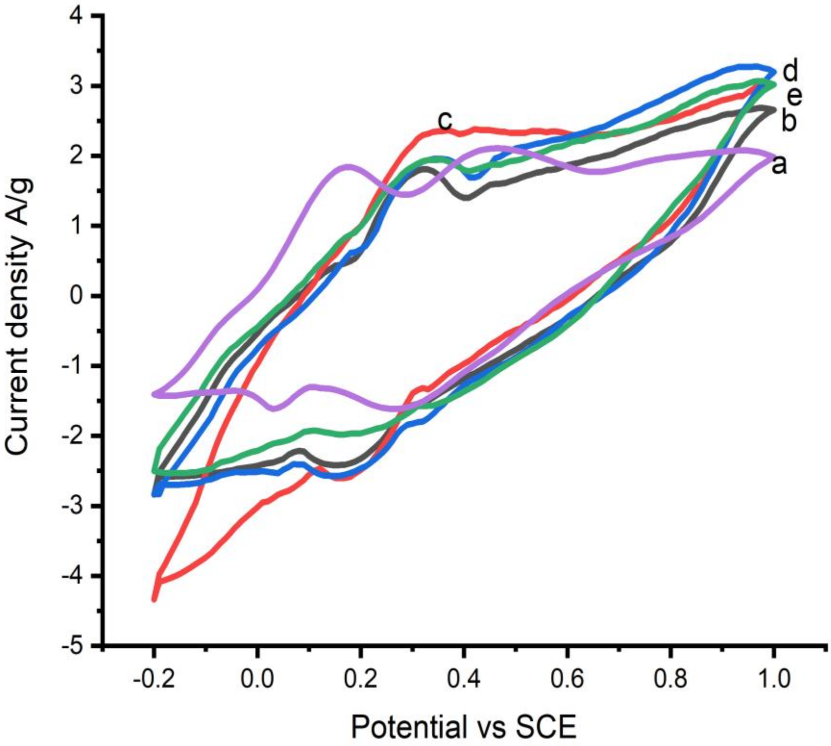

Fig: 3.9 CV of (a) PANI (b) PANI-La_2O_3-0.1, (c) PANI-La_2O_3-0.2, (d) PANI-La_2O_3-0.3, (e)) PANI-La_2O_3-0.5.

CV of PANI shows two pair of clear redox peaks which confirms the pseudo capacitive behavior of PANI. These redox peaks reveal the redox transition between leucoemeraldine and protonated emeraldine salt and between emeraldine and pernigraniline. The oxidization peak at about 0.18 V is due to the transformation of the leucoemeraldine to conductive emeraldine salt form. The oxidization peak at 0.42 V corresponds to the transformation of emeraldine oxidation state to fully oxidized pernigraniline state.The reduction peaks at 0.03 V and 0.25 V are due to the transformation of leucomeraldine and emeraldine base respectively.

The lanthanum oxide doping leads to the shifting of redox peaks of PANI to higher potential in anodic sweep and lower to lower potential in the cathodic sweep. The increase in the concentration of the oxide leads to the more shift in redox peaks to higher potential and increase in area of cyclic voltagram. This is supposed to stem from combine contribution of both lanthanum oxide and PANI. The graph shows that the electrochemical behavior of the sample materials depends on the concentration of dopant used. CV of the doped samples shows good redox current, the sample PANI-La_2O_3-0.2 has good redox current in comparison to others this is probably due to appropriate combination of the oxide and PANI. PANI-La_2O_3-0.2 has oxidation peaks at 0.33 and 0.41, reduction peaks at 0.17 and 0.34.

The specific capacitance value thus calculated from the CV curve is shown in table 3.

Table 1: Specific Capacitance of various samples of PANI-La_2O_3

Samples	Specific capacitance (Fg^{-1})
PANI	135
PANI-La_2O_3-0.1	163
PANI-La_2O_3-0.2	206
PANI-La_2O_3-0.3	185
PANI-La_2O_3-0.5	170

The table 3 shows out of these four samples prepared at room temperature, PANI-La_2O_3 0.2 has highest specific capacitance of 206 Fg^{-1}.

3.6.2 Galvano static Charge- Discharge Curve (GCD)

The Fig. 3.10 (a)shows the charge /discharge profile is asymmetrical for PANI due to the redox reaction at electrode/electrolyte interface, these asymmetrical triangular shapes points the Pseudo capacitive behavior.

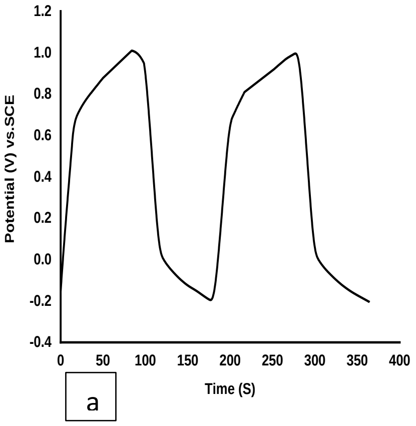

a

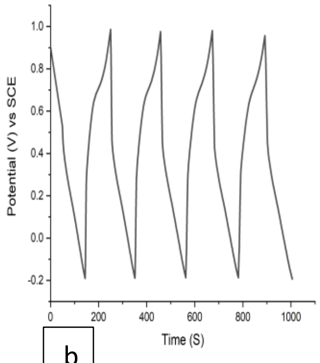

b

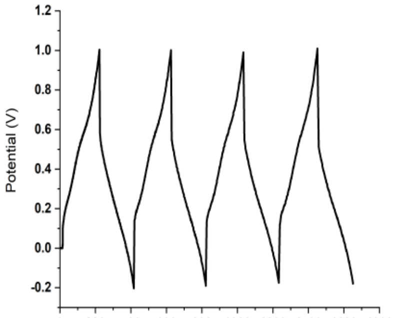

c

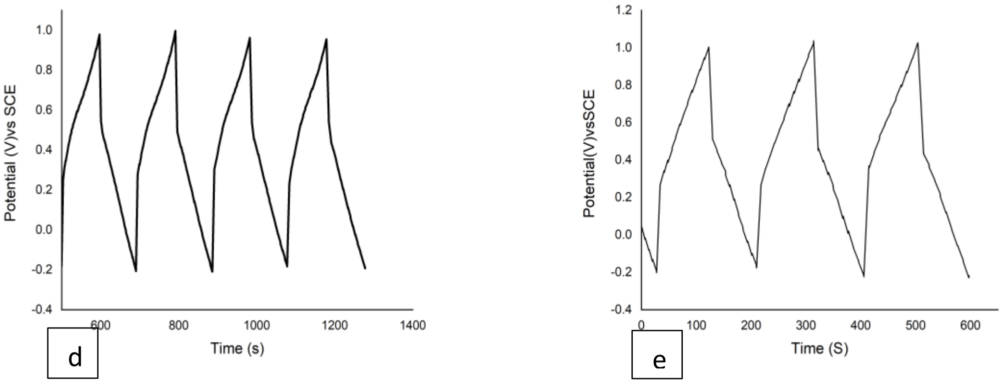

Fig: 3.10 GCD curves (a) PANI (b) PANI-La_2O_3-0.1 (c) PANI-La_2O_3-0.2 (d) PANI-La_2O_3-0.3 (e) PANI-La_2O_3-0.5

The value of SC for PANI is found to be 145 Fg^{-1} at current density of 2 Ag^{-1}.In the same Fig. 3.10 (b), (c), (d) and (e) shows the charge discharge graphs of the different PANI-La_2O_3 composites with varying amount of oxide at current density of 2 Ag^{-1} with potential window of -0.2 V to 1 V the flattening of the graphs of these composites points the pseudo capacitive nature due to the redox reaction at electrode/electrolyte interface. The higher capacitance of 206 Fg^{-1} was found for PANI-La_2O_3-0.2 composite among all.

The specific capacitance, energy density and power density of active materials are calculated and tabulated in table 4.

Table 2: Specific Capacitance of samples obtained from charge discharge cycles

Samples	Specific capacitance (Fg^{-1})	Energy density $WhKg^{-1}$	Power Density WKg^{-1}
PANI	145	7.25	284
PANI-La_2O_3-0.1	163	8.15	299.38
PANI-La_2O_3-0.2	210	10.5	300
PANI-La_2O_3-0.3	155	7.75	300
PANI-La_2O_3-0.5	153	7.65	299.34

The specific capacitance obtained from both CV and GCD follows the same trends and the PANI-La_2O_3 0.2 sample has found to have the highest specific conductance, energy density and reliable power density could be the best material for super capacitor application.

3.6.3 Cycle Life Test and Coulombic Efficiency Measurement

Cycle Life Test and Coulombic Efficiency Measurement of the best sample were performed. Fig. 3.11 shows the retention capacity of the PANI-La_2O_3-0.2 after1000 cycles.

Coulombic efficiency η was calculated by using the relation:

$$\eta = \frac{\mathrm{td}}{tc} \times 100\ \% \quad \ldots\ldots\ldots\ldots\ldots\ldots\ldots\ldots\ldots\ldots\ldots\ldots\ldots \ (3.1)$$

Where, td represents discharging time while tc represents the charging time. The Coulombic efficiency η is found to be 89.85% at current density of 2 Ag^{-1}.

The life cycle retention was calculated using an equation:

$$\text{Retention percentage} = \frac{Sc\ of\ cycle}{Sc\ of\ first\ cycle} \times 100 \ldots\ldots\ldots\ldots\ldots\ldots\ldots\ldots (3.2)$$

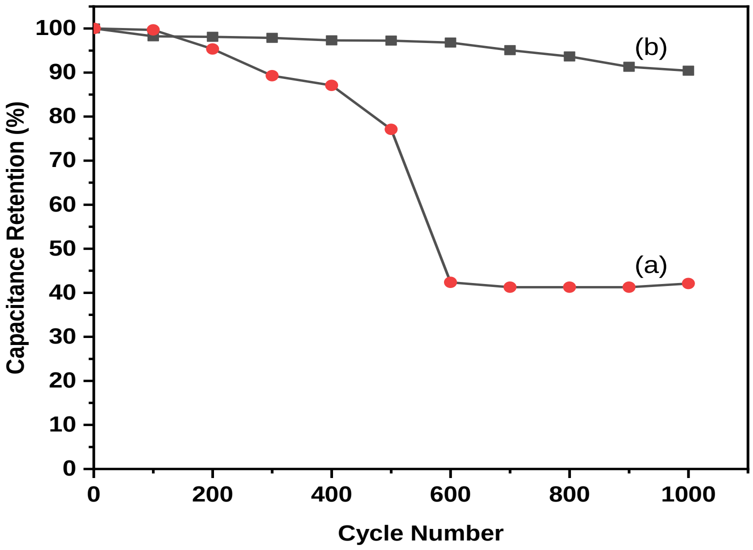

Figure: 3.11 variation of specific capacitance with cycle number of sample (PANI-La_2O_3-0.2) 1000 Cycles at scan rate of 20 mV/s.

For cyclic stability CV of 1000 cycles were performed at scan rate of 200 mV/s it was found that specific capacitance of 1000 cycles become 91.17% of initial cycle for composite and 42.6% for the PANI.

3.6.4 Two electrode system

The electrochemical characterization of the best sample, CV and GCD was also performed by two electrode system by using two electrodes of same composites having same mass and surface area, using the same electrolyte used in three electrode system, the results are shown in Fig. 3.12. The capicatance obtained by two electrode system is found to be nearly four times less that of the three electrode system. The specefic capacitance from CV is found to be 47 Fg^{-1} and that from GCD is 49 Fg^{-1}.

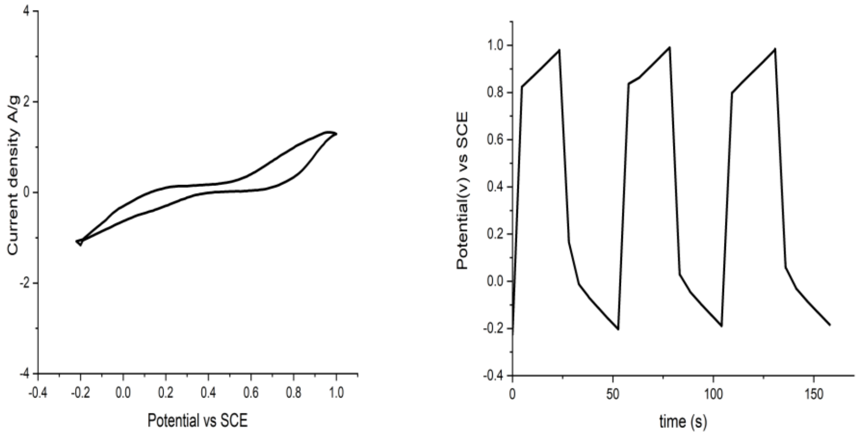

Fig: 3.12 (a) CV of two electrode system (b) GCD of two electrode system

CHAPTER-4: CONCLUSIONS AND SUGGESTIONS FOR FURTHER WORK

4.1 CONCLUSIONS

In this study aniline was polymerized by aqueous oxidative chemical polymerization method, using ammonium persulphate as an oxidant in 1M H_2SO_4 solution. The oxidative polymerization of aniline was performed at room temperature. The polyaniline was doped with different concentration of metal oxides to study the effect of concentration of dopants on conductivity and specific capacitance of prepared materials. Composite of various sample of PANI was mixed with carbon powder and PVDF and fed into nickel form for the preparation of electrode to study electrochemical properties such as CV and charge discharge cycle. Electrochemical measurements like cyclic voltammetry and charge-discharge curve of the composite materials were studied which shows that the specific capacitance for the sample (S_2) 0.2 La_2O_3 doped in PANI in 1M H_2SO_4 has highest values of 206 Fg^{-1} is obtained from CV; this may be due to formation of more active sites over the surface of composite material in comparison to others. The charge discharge curve shows a regular symmetric charging and discharging line which explains good reversible nature of the PANI-La_2O_3 The specific capacitance values for samples calculated from charge discharge curve have same trend as those calculated from CV curve and highest value was 210 Fg^{-1} for sample (S_2) 0.2 La_2O_3 doped PANI in 1M H_2SO_4 The energy density of 10.5 $WhKg^{-1}$ and power density of 300 WKg^{-1}. Based on the properties shown, this work could be could be the helpful for pseudo capacitors application.

4.2 SUGGESTIONS FOR FURTHER WORK

Lanthanum oxide doped polyaniline electrode is promising material for the super capacitor applications. Hence further research and additional development in this electrode materials guide to enhance the better performance of supercapacitor. Some of them are as follows.

1. Size of the nanoparticles play important role in the supercapacitors applications so it should reduce and study.

2. The salt-based aqueous electrolyte such as Na_2SO_4, K_2SO_4, Li_2SO_4 which are economically available should be examined in future works for electrochemical measurements.
3. Electrochemically active additives should be searched to enhance the capacitance of the electrode.
4. The electrode materials binder with low resistance and high conductivity should be research to enhance the electrode performance.

REFERENCES

1. Qi, Zhaoxiang; Koenig and Gary M., Journal of Vacuum Science & Technology B, Nanotechnology and Microelectronics: Materials, Processing, Measurement, and Phenomena, **2017,** *35(4),* 040801
2. Tehrani Z., Thomas D.J. and Korochkina T., Phillips C.O., Lupo, D., Lehtimäki, S.O., Mahony J. and Gethin D.T., *Energy,* **2017** *118, 1313-1321*
3. Bueno, Paulo R., *Journal of Power Sources,* **2019.**
4. Marin S., Halper J., and Ellenbogen C., MITRE Nanosystems Group, http://www.mitre.org/tech/nanotech MP 05W0000272, **2006,** 48
5. Conway B. E., Electrochemical Supercapacitors: Scientific Fundamentals and Technological Applications. New York, Kluwer-Plenum, **1999**, 234-267.
6. Arico A. S. and Bruce P., *Nature Materials*, **2005**, *4*, 366-377.
7. Conway B. E., *Journal of the Electrochemical Society,* **1991**, *138(6*), 1539 - 1548
8. Lee K. Y. T., *A Thesis Submitted for the Degree of Master of Applied Science Graduate Department of Mechanical and Industrial Engineering University of Toronto, **2014***, 88-90
9. Arico A. S. and Bruce P., *Nature Materials*, **2005**, *4*, 366-377
10. Bajwa G., A, *Thesis Submitted for the Degree of Master of Applied Science Graduate Department of Mechanical and Industrial Engineering University of Toronto,* **2012,**
11. Aguirre C. J., Ferreira A., Ding H, Samson A. J., Kopidakis N. Asta M., Pilon L., Rubin Y. Tolbert H. S., Schwartz J. B., Dunn B and Ozolins V., *Journal of Physical Chemistry* **2014**, *118*, 19505−19523
12. Sniechowski M., *A Dissertation (Ph.D.) Submitted to Faculty of Physics and Applied Computer Science, University Joseph Fourier*, **2005**, 1-152.
13. Jayalakshmi M. and Balasubramanian K., *Journal of Electrochemical Science*, **2008**, *3*, 1196
14. Conway B. E. and Birss V., *Journal of Power Sources***, 1997**, *66(1-2)*, 1-14.
15. Mastragostino M. and Arbizzani C., *Journal of Power Sources*, **2001** *97(8),* 812-815

16. Ryu K. S. and Kim K. M., *Journal of Power Sources***, 2002,** *103(2),* 305-309.
17. The Royal Swedish Academy of Sciences, Information Department, Web site: www.kva.se,The Nobel Prize in Chemistry, ***2000.***
18. Kinlen P. J., Ulyanova Y. V. and Rawlings G. D., *Materials and Processes,* **2005**, *1*, 243-248
19. Frackowiak E. and Khomenko V., *Journal of Power Sources,* **2005***, 32(2),* 62-67.
20. Tharani S and Chidambara Vinayagam, *International Journal of Advanced Research* **(2015**), 3, *(3)* 810-822.
21. Li L., Loveday D.C., Mudigonda D.S.K., Ferraris J.P., Cantero I., *Journal of Electro chemistry communication Society*., **2002** *149*, A1201–1207.
22. Ryu K.S., Kim K.M., Park N.G., Park Y.J. and Chang, S.H., *Joural Power Sources*, **2002,** *103*, 305–309.
23. Bian C., Yu A., Wu H., *Journal of Electro chemistry communication*., ***2011****: 266–269.*
24. Xie S., Gan M., Ma L., Li, Z., Yan, J., Yin H., Shen X., Xu F., Zheng J. and Hu, J., *Electrochim. Acta***, 2014,**120: 408–415
25. Hu, Z.A., Xie, Y.L., Wang, Y.X., Mo, L.P., Yang, Y.Y. and Zhang, Z.Y. *Mater.Chem. Phys*.**2009**, *114*, 990–995
26. Michaelson and Jeff C, Endeavour, **1993**, *17(3)* 121-126.
27. Liu G., *A Master Thesis Submitted to Institute of Chemistry*, Lehigh University, **1997**, University Paper 497.
28. Harima Y., Patil R., Yamashita K., Yamamoto N., Ito S. and Kitan A., Chemical Physics Letter, **2001**, *345*, 239-244.
29. MacDiarmid A. G. and Epstein A. J., Faraday Discussions of the Chemical Society **1989**, *88*, 317-332.
30. Palaniappan S. and Nivasu V., *New Journal of Chemistry*, **2002**, *26,* 1490-1494
31. Sniechowski M., Anna P. G. and Pielichowski *Journal of Polymer Bulletin*, **2011**, *66*, 863-869.
32. Albuquerque J. E., Mattoso L. H. C., Balogh D. T., Faria R. M, Masters J.G. and MacDiarmid A.G., *Synthetic Metals*, **2000**,*113*, 19-22.

33. Zor S. and Yakar E., Bulletin of Electrochemistry, **2007**, *23*, 149–153.
34. Stejskal J., Sapurina I. and Trchová M., *Progress in Polymer Science,* **2010**, *35*, 1420–1481.
35. Devkota N.B., *A Dissertation Submitted for the Master of Science Degree in Chemistry, Tribhuvan University, Nepal*, **2014**, 04-15.
36. Dhawan S.K., Ram M.K., Malhotra B.D. and Chandra S., *Synthetic Metals,* **1995,** *75*, 119-122.
37. Shah A. A., A Master Thesis Submitted to Institute of Chemistry, Chemnitz University of Technology, **2007**, 1-123
38. Lanthanum Oxide. *American Elements*, **2018**.
39. Shang G., Peacock P. W., Robertson J., *Applied Physics Letters*, **2004,** *84 (1)*, 106–108.
40. Wells A.F., *Structural Inorganic Chemistry,* **2004,** 46.
41. Wyckoff, R. W.G, Crystal Structures, **1963.**
42. Kale S.S., Jadhav, K.R., Patil, P.S., Gujar, T.P and Lokhande C.D, *Materials Letters*, **2005 59** (24–25), 3007–3009.
43. Vinogradova N. N., Dmitruk L. N., Petrova O. B., *Glass Physics and Chemistry*, **2004,** *30*, 1–5.
44. Cao J., Ji H., Liu J., Zheng M., Chang X., Ma X., Zhang A. and Xu Q. *Materials Letters*, **2005,** *59 (4)*, 408–411.
45. O.V. Manoilova, *Journal of physical chemistry B*, **2004**, *108 (40*), 15770–15781.
46. Khilari S.,Pandit S.,Varnasi J.L., Das D. and Pradhan D. *Journal of American Chemical Society Applied Materials Interface*, **2015,***7(20)*, 6578-20666**.**
47. Rasmchandran R.,ChenS.M., Peter G.and Kumar G.International Journal of Electrochemical Science **2015**,1o,7111-7137.
48. US 2800616, Becker, H.I., Low voltage electrolytic capacitor, ***1957***, *07-23*
49. *Ho, J.; Jow, R.; Boggs, S.,IEEE Electrical Insulation Magazine* **2010, *26*** *(1,)20–1.4*
50. A brief history of supercapacitors AUTUMN 2007 Batteries & Energy Storage Technology Archived **2014**-01-06 at the Wayback Machine.

51. US 3288641, Rightmire, Robert A.,Electrical energy storage apparatus, **1966**, 11-29
52. J. G. Schindall, *IEEE Spectrum*, **2007.**
53. Conway, B.E., *Scientific Fundamentals and Technological Applications (in German), Berlin, Germany*: *Springer,* **1991**–*8,* ISBN 978-0306457364
54. Conway, B. E., *Journal of Electrochemical Society*, **1991**, *138 (6),* 1539–154.
55. David A. E., *Containers with anodes and cathodes with electrolytes ,* **1994**, 11-29
56. David A., *In Proceedings of the 14th Capacitor & Resistor Technology Symposium,* **1994**
57. Evans Capacitor Company, *Capattery series,* **2007.**
58. W.C., Wen T.C., Teng H., *Electrochim. Acta*, **2003**, *48*, 641-650
59. Bigg D. M., Bradbury E. J., *Conducting Polymers Plenum Press*, New York, **1981,**
60. Clark J. C., Ihas G. G., Reghu M., Yoon C. O., Heeger A. J., Cao Y., Journal of *Low Temperature Physics*, **1995**.
61. Surville R.D., Jozefowicz M., Yu L.T., Pepichon J., *ElectrochemActa*., **1968,** *13(6)*, 1451-1458.
62. Haung W. S., Humphery B. D., Mac Diarmid A. G., *Journal of Chemical Society Faraday Trans I.* **1986.**
63. Gustafsson A.J., *Journal of Electronics*, 1**992**.
64. Song R.Y., Park J.H., Sivakkumar S.R., Kim S.H., Ko J.M., Park D.Y., Jo S.M., Kim D.Y. *Journal of Power Sources,* **2007**
65. Yang M., Cheng B., Song H., Chen X., *Electrochim Acta*, **2010**.
66. Zhou Y., Qin Z.Y., Li L., Zhang Y., Wei Y.L., Wang L.F., Zhu M.F., *Electrochim Act*a**, 2010**
67. Wang H., Hao Q., Yang X., Lu L., Wang X., *Electrochemical Communication*, **2009**, *11* 1158-1169.
68. Mujawar H.S., Ambade S.B., Battumu T., Ambade R.B., Lee S.H., Electrochim. Acta **2011,** *56,* 4462-4468
69. Chen L., Sun L.J., Luan F., Liang Y., Li Y., Liu X.X., *Journal of Power Sources,***2010,** *195,* 3742-3748.

70. Patil K. S., Zope P. H., *International journal of engineering sciences & research technology*,http: //www.ijesrt.com, 2015, ISSN: 2277-9655: 3.785
71. Yang M., *ElectrochimicaActa.*, **2010,** 55, 7021–7027.
72. Trend, Raissa M., and Brian M. Stoltz., *Journal of the American Chemical Society,* **2004**,126 (14), 4482-4483.
73. Gui-wen, H, *Jiangxi Metallurgy*, **2003**, *23(6)*, 62-68.
74. Rahul R. S., Shao H., Kelvin C., Wu Y. Y., *Chemsus Chem,* **2014**, 125.
75. Streeter, J., Schickling, B. M., Jiang, S., Stanic, B., Thiel, W. H., Gakhar, L. & Miller Jr, F. J, *Circulation research*, 115(11), 911-918.
76. Tsushima, S., & Hirai, S., *Journal of Thermal Science and Technology*, **2015**, *10(1),* JTST0002-JTST0002.
77. Dhahri, A., Jemmali, M., Dhahri, E., & Valente, M. A., Journal of Alloys and Compounds, **2015**, *638*, 221-227.
78. Wang H., & Pilon L. J., *Electrochimical Acta***,** ***2012***, *76, 529-531.*
79. Lassoued, A., Dkhil, B., Gadri, A., & Ammar, S., Results in physics, **2017**, *7*, 3007-3015.
80. Park, A. R., Jeon, K. J., & Park, C. M., *Electrochimica Acta,* **2018**, *265, 107-114.*
81. Li, X. X., Tian, D., He, C. H., & He, J. H, *Electrochimica Acta*, **2019**, 296, 491-493.
82. Orapan L. Ekkkasit P., Unchalee S., Dussadee R. B., *University international conference* , **2013.**
83. Gul S., Anwar-ul-Haq S. A. and Bilal S., *Journal of Chemistry*, **2015**, 10, 1155
84. Wang D., Ni W., Pang H., *Electrochim Acta*, **2010**, *55*, 6830-6835.
85. N. Sulaiman*, American Institute of Physics,* **2018**, 020105.
86. Koirala K., *A Dissertation Submitted for the Master of Science Degree in Chemistry, Tribhuvan University, Nepal,* **2014**, 04-1586